The COOH-Terminal Domain of Myo2p, a Yeast Myosin V, Has a Direct Role in Secretory Vesicle Targeting

Daniel Schott, Jackson Ho, David Pruyne, and Anthony Bretscher

Department of Molecular Biology and Genetics, Cornell University, Ithaca, New York 14853

Abstract. *MYO2* encodes a type V myosin heavy chain needed for the targeting of vacuoles and secretory vesicles to the growing bud of yeast. Here we describe new *myo2* alleles containing conditional lethal mutations in the COOH-terminal tail domain. Within 5 min of shifting to the restrictive temperature, the polarized distribution of secretory vesicles is abolished without affecting the distribution of actin or the mutant Myo2p, showing that the tail has a direct role in vesicle targeting. We also show that the actin cable–dependent translocation of Myo2p to growth sites does not require secretory vesicle cargo. Although a fusion protein containing the Myo2p tail also concentrates at growth sites, this accumulation depends on the polarized delivery of secretory vesicles, implying that the Myo2p tail binds to secretory vesicles. Most of the new mutations alter a region of the Myo2p tail conserved with vertebrate myosin Vs but divergent from Myo4p, the myosin V involved in mRNA transport, and genetic data suggest that the tail interacts with Smy1p, a kinesin homologue, and Sec4p, a vesicle-associated Rab protein. The data support a model in which the Myo2p tail tethers secretory vesicles, and the motor transports them down polarized actin cables to the site of exocytosis.

Key words: cell polarity • myosin V • *MYO2* gene product • exocytosis • *Saccharomyces cerevisiae*

ESSENTIALLY all eukaryotic cells are polarized, from single cell fungi to animal cells in tissues. This polarity is reflected in polarized microtubule and microfilament cytoskeletons and polarized membrane transport (for reviews see Drubin and Nelson, 1996; Keller and Simons, 1997). In animal cells, long-range vesicle transport occurs along microtubules using kinesin motors, and then switches to short-range myosin-driven transport along actin filaments near the final delivery site (for review see Schliwa, 1999). Similarly, in filamentous fungi, both microtubules and actin direct polarized secretion (for reviews see Heath, 1994; Seiler et al., 1997). In contrast, microtubules play no role in polarized secretion in the yeast *Saccharomyces cerevisiae* (Jacobs et al., 1988; Huffaker et al., 1988).

Nevertheless, actin is essential for polarized secretion, which directs growth in yeast, and as a result, cells with defective actin cannot bud but instead become enlarged spheres which expand isotropically (Novick and Botstein, 1985). Accordingly, the actin cytoskeleton consists mainly of cortical actin patches concentrated near regions of growth and cables oriented towards the same regions (Adams and Pringle, 1984). For example, in small-budded cells, actin patches congregate in the growing bud and cables extend from the mother cell into the bud.

Until recently it was uncertain whether cortical patches, actin cables, or both direct secretion. The isolation of the conditional tropomyosin mutant *tpm1-2 tpm2Δ* has resolved this issue (Pruyne et al., 1998). Upon shifting to the restrictive temperature, tropomyosin-containing actin cables disappear within a minute, followed by the depolarization of the secretory vesicle marker Sec4p within the next minute, even though actin patches remain polarized for >15 min. Shifting depolarized cells back to the permissive temperature restores cables and polarized Sec4p within 1 min and budding within 10 min, although actin patches do not repolarize until 15 min. These results show that actin cables direct secretory vesicle delivery independently of the actin patch distribution.

One protein whose distribution responds rapidly to actin cable disassembly and reassembly is Myo2p (Pruyne et al., 1998), a myosin V needed for polarized delivery of secretory vesicles and vacuole membranes (Johnston et al., 1991; Govindan et al., 1995; Hill et al., 1996; Santos and Snyder, 1997; Catlett and Weisman, 1998). Myo2p normally concentrates at the same sites of exocytosis and growth as secretory vesicles and Sec4p (Lillie and Brown, 1994; Walch-Solimena et al., 1997).

Myosin Vs are double-headed myosins with a conserved

Address correspondence to Anthony Bretscher, Department of Molecular Biology and Genetics, 351 Biotechnology Building, Cornell University, Ithaca, NY 14853. Tel.: (607) 255-5713. Fax: (607) 255-2428. E-mail: apb5@cornell.edu

globular domain (or tail) of poorly understood function at the COOH terminus, separated from the NH_2-terminal actin-binding motor domain by a coiled–coil dimerization domain (Cheney et al., 1993) (see Fig. 1). In animal cells, myosin V transports membranes (for review see Mermall et al., 1998), leading to a model for membrane transport in which the tail binds to cargo while the motor walks along actin filaments (see Prekeris and Terrian, 1997). However, some observations do not seem to fit such a simple model for Myo2p. First, the original conditional *myo2* allele, *myo2-66*, causes severe defects in the actin cytoskeleton (Johnston et al., 1991), suggesting that Myo2p might polarize secretion indirectly through its effect on the cytoskeleton. Second, the continued partial localization of Myo2p in the apparent absence of actin filaments (Ayscough et al., 1997), and recent evidence that the tail may affect the polarized distribution of Myo2p (Catlett and Weisman, 1998; Reck-Peterson et al., 1999) have been interpreted to mean that it is the tail, not the motor, that directs Myo2p to growth sites.

We describe two approaches to investigate the role of the Myo2p tail. First, we made conditional lethal mutations in this putative cargo-binding domain, and second, we expressed fusion proteins containing the cargo-binding domain. Both approaches show that the tail's primary function is to carry secretory cargo.

Materials and Methods

Temperature-sensitive myo2 Yeast Strains

Table I lists the yeast strains and Table II the plasmids used. Sherman (1991) and Ausubel et al. (1996) describe the methods used for growth, maintenance, and genetic manipulation of yeast, and Gietz and Schiestl (1995) describe the method used to transform yeast.

Temperature-sensitive *myo2* strains were generated by replacing the 3′ region of the endogenous genomic *MYO2* gene with mutagenized plasmid DNA. To construct a plasmid capable of integrating 3′ to *MYO2*, pJP10-2B (YCp50 containing *MYO2*) (Johnston et al., 1991) was cut with SpeI and the resulting fragments circularized using T4 DNA ligase. The ligated DNA served as template for five cycles of amplification by PCR using *Taq* DNA polymerase and the oligonucleotide primers GATAATGAAATCGATATTATGGAAGA and CGGGATCCATTATCATACTATACTATTGACAAATACTTC. The ClaI-BamHI segment of the 1.7-kb product was inserted into pRS303 (Sikorski and Hieter, 1989). Destruction of the pRS303 SpeI site by cutting with SpeI (partial digest) and XbaI and religation produced the plasmid pRS303MYO2, containing the 201-bp ClaI-SpeI fragment of the *MYO2* 3′ untranslated region, followed by the 1,587-bp segment of *MYO2* from the SpeI site at +3271 on, fused to the sequence GCACTAGA and the NotI site of pRS303.

pRS303MYO2 served as a template for PCR-based mutagenesis (Cadwell and Joyce, 1992), modified to reduce the mutation frequency. The reaction mix (1 mM dCTP, 1 mM dTTP, 0.2 mM dATP, 0.2 mM dGTP, 40 ng pRS303MYO2 cut with PvuII, 7 mM $MgCl_2$, 0.5 mM primers, 50 mM KCl, 10 mM Tris-HCl, pH 8.3, 10 mg BSA, and 0.05% Tween 20; and after the mix had warmed up to 80°C, 0.3 mM $MnCl_2$ and 5u *Taq* DNA polymerase) was subjected to six cycles of amplification and the EcoRI-NotI fragment of the PCR product was subcloned into the corresponding re-

Table I. Yeast Strains

Name	Genotype	Source
ABY530	*MATα myo2-20::HIS3 his3-Δ200 ura3-52 leu2-3,112 lys2-801 ade2-101* Gal+	This study
ABY531	*MATα MYO2::HIS3 his3-Δ200 ura3-52 leu2-3,112 lys2-801 ade2-101* Gal+	This study
ABY532	*MATα myo2-12::HIS3 his3-Δ200 ura3-52 leu2-3,112 lys2-801 ade2-101* Gal+	This study
ABY533	*MATα myo2-13::HIS3 his3-Δ200 ura3-52 leu2-3,112 lys2-801 ade2-101* Gal+	This study
ABY534	*MATα myo2-14::HIS3 his3-Δ200 ura3-52 leu2-3,112 lys2-801 ade2-101* Gal+	This study
ABY535	*MATα myo2-66::HIS3 his3-Δ200 ura3-52 leu2-3,112 lys2-801 ade2-101* Gal+	This study
ABY536	*MATα myo2-16::HIS3 his3Δ200 ura3-52 leu2-3,112 lys2-801 ade2-101* Gal+	This study
ABY537	*MATα myo2-17::HIS3 his3-Δ200 ura3-52 leu2-3,112 lys2-801 ade2-101* Gal+	This study
ABY538	*MATα myo2-18::HIS3 his3-Δ200 ura3-52 leu2-3,112 lys2-801 ade2-101* Gal+	This study
ABY551	*MATa MYO2::HIS3 his3-Δ200 ura3-52 leu2-3,112 lys2-801 ade2-101* Gal+ *MATα MYO2::HIS3 his3-Δ200 ura3-52 leu2-3,112 lys2-801 ade2-101*	This study
ABY553	*MATa myo2-16::HIS3 his3-Δ200 ura3-52 leu2-3,112 lys2-801 ade2-101* Gal+ *MATα myo2-16::HIS3 his3Δ200 ura3-52 leu2-3,112 lys2-801 ade2-101*	This study
ABY555	*MATa myo2-66::HIS3 his3-Δ200 ura3-52 leu2-3,112 lys2-801 ade2-101* Gal+ petite *MATα myo2-66::HIS3 his3-Δ200 ura3-52 leu2-3,112 lys2-801 ade2-101*	This study
ABY988	*MATa tpm1-2::LEU2 leu2-3,112 tpm2Δ::HIS3 his3-Δ200 ura3-52 lys2-801 SEC8:HA3::TRP1 trp1-1* *MATα tpm1-2::LEU2 leu2-3,112 tpm2Δ::HIS3 his3-Δ200 ura3-52 lys2-801 SEC8:HA3::TRP1 trp1-1*	Pruyne et al., 1998
ABY1128	*MATa tpm1-2::LEU2 leu2-3,112 tpm2Δ::HIS3 his3-Δ200 myo2-16::URA3 ura3-52 lys2-801 trp1-1* *MATα tpm1-2::LEU2 leu2-3,112 tpm2Δ::HIS3 his3-Δ200 myo2-16::URA3 ura3-52 lys2-801 trp1-1*	This study
DBY2000	*MATα act1-1 ura3-52*	D. Botstein
HMSF134	*MATa sec5-24*	R. Schekman
HMSF143	*MATa sec9-4*	R. Schekman
JP7B	*MATa myo2-66 his3-Δ1 ura3-52 leu2-3,112 ade1 trp1-289*	D. Carruthers
NY3	*MATa sec1-1 ura3-52*	P. Novick
NY13	*MATa ura3-52*	P. Novick
NY17	*MATa sec6-4 ura3-52*	P. Novick
NY130	*MATa sec2-41 ura3-52*	P. Novick
NY405	*MATa sec4-8 ura3-52*	P. Novick
PSY316	*MATα his3-Δ200 ura3-52 leu2-3,112 lys2-801 ade2-101* Gal+	P. Schatz
RSY786	*MATα sec2-56 ura3-52 leu2-3,112*	R. Schekman

Table II. Plasmids

Name	Type	Auxotrophic marker	Other features	Source
pJP10-2B	centromere/ARS (low copy number)	*URA3*	*MYO2*	Johnston et al. (1991)
pRS303MYO2	integrating	*HIS3*	Integrates 3′ to *MYO2*	This study
pRS303myo2^{ts}	integrating	*HIS3*	Integrates 3′ to *MYO2*, replacing wild-type sequence with *myo2^{ts}*	This study
pRS306myo2^{ts}	integrating	*URA3*	Integrates 3′ to *MYO2*, replacing wild-type sequence with *myo2^{ts}*	This study
YEpSMY1	2μ circle (high copy number)	*LEU2*	SMY1	This study
pEG	2μ circle (high copy number)	*URA3, leu2d*	GST expressed from *GAL* promoter	Mitchell et al. (1993)
pEGM	2μ circle (high copy number)	*URA3, leu2d*	GST fused with Myo2p tail, expressed from *GAL* promoter	This study
pCG	centromere/ARS (low copy number)	*URA3*	GST expressed from *GAL* promoter	This study
pCGM	centromere/ARS (low copy number)	*URA3*	GST fused with Myo2p tail, expressed from *GAL* promoter	This study
pCL	centromere/ARS (low copy number)	*URA3*	LexA expressed from *GAL* promoter	This study
pCLM	centromere/ARS (low copy number)	*URA3*	LexA fused with Myo2p tail, expressed from *GAL* promoter	This study

gion of pRS303MYO2 to make libraries of mutagenized *MYO2*. When cut with SpeI and transformed into yeast, the library plasmids insert pRS303 (containing *HIS3*) into the ClaI site of the *MYO2* 3′ untranslated region, and replace the EcoRI-ClaI region of *MYO2* with mutagenized sequence encoding amino acid residues 1119 to the COOH terminus.

Roughly 500 transformants at 30°C were replica-plated to 14 and 37°C to detect conditional-lethal mutants. Phloxine B included in plates at 10 mg/liter allowed easier identification of growth-arrested yeast (Horn and Wilkie, 1966). Because dead cells absorb this red dye, red marks correspond to the positions of temperature-sensitive colonies. Genomic DNA from each of the temperature sensitives was cut with SpeI and circularized to reconstitute versions of pRS303MYO2 containing mutations. Transformation of these plasmids relinearized with SpeI into the yeast strain PSY316 yielded the temperature-sensitive strains ABY532, 533, 534, 536, 537, 538, and 530. The temperature sensitivity could be complemented by transformation with pJP10-2B (*MYO2* on a low copy number plasmid) or by mating with a *MYO2* strain, but could not be complemented by mating with JP7B, a *myo2-66* strain. ABY531, an isogenic *MYO2* strain, was made by transformation of PSY316 with pRS303MYO2. An analogous series of plasmids made from pRS306 (containing *URA3*) allowed the construction of yeast strains containing *myo2* alleles tagged with *URA3*. To make an isogenic *myo2-66* strain, genomic DNA from JP7B transformed with pRS303MYO2 was cut with NcoI and religated, resulting in an integrating plasmid analogous to pRS303MYO2, but containing the full-length *myo2-66* gene instead of the *MYO2* fragment. This plasmid was cut with NcoI and transformed into PSY316 to construct ABY535. Diploid versions of these strains were made by transiently transforming with YCp50HO, a plasmid bearing *HO* (Herskowitz and Jensen, 1991).

Genetic Interactions of myo2^{ts} Alleles

Genetic interactions of *myo2-13* with *sec1-1*, *sec2-56*, *sec5-24*, *sec6-4*, and *sec9-4* mutations were tested by mating ABY533 with *MATa sec^{ts}* strains (*MATa* strains being generated from *MAT*α by standard genetic methods), sporulating, and dissecting tetrads onto synthetic minimal dextrose medium (SD)[1] and yeast extract peptone-dextrose medium (YPD) at 30°C. Crosses producing a high frequency of tetrads with four viable spores are considered not to show synthetic lethality. $P < 0.05$ in all cases reported and $P < 0.0005$ in most cases, based on a binomial distribution, assuming meiotic gene conversion does not exceed 20%. Nonsynthetic lethals were confirmed by testing temperature sensitivity to show that some viable spores are likely to be *myo2-13 sec^{ts}* double mutants. We suspected that *myo2-13* is synthetically lethal with *sec4-8* but could not prove it by the method described above, because even *MYO2^{+}* strains have low spore viability when crossed with the *sec4-8* strain NY405. Therefore, we determined synthetic lethality of *sec4-8* with *myo2^{ts}* mutations by constructing *sec4-8 myo2^{ts}* strains bearing pJP10-2B, a *CEN* plasmid containing *MYO2* and *URA3*. Strains with synthetic lethal combinations are unable to grow at 22°C on minimal medium containing 5-fluoro-orotic acid, which selects against *URA3*. To determine synthetic growth defects of nonlethal combinations, restrictive temperatures with and without pJP10-2B were compared. At least three different strains from the *sec4-8* × *myo2^{ts}* cross were tested for each combination of alleles and conditions.

To screen for overexpression suppressors of *myo2^{ts}*, *myo2-17*, *myo2-18*, and *myo2-20* strains were transformed with a multicopy (2μ) genomic library in YEp351 (Engebrecht et al., 1990), and 287,000 colonies replica-plated onto rich media at 37°C. *SMY1* was isolated from one clone by subcloning the PstI-StuI fragment of the insert into PstI-SmaI of YEp351. YEpSMY1, the resulting plasmid, contains the *SMY1* open reading frame flanked by the 5′ 651 bp and 3′ 266 bp of untranslated sequence.

Fluorescence Microscopy

To produce anti-Myo2p antibodies, the NsiI-EcoRI fragment of pJP10-2B, encoding amino acid residues 784–1118 of Myo2p (encompassing the IQ repeat and coiled–coil domains), was subcloned into pRG32D (Gary and Bretscher, 1995) and the glutathione *S*-transferase (GST)–Myo2p fusion protein was purified as described (Smith and Johnson, 1988) (Amersham Pharmacia Biotech). Rabbit antisera against the fusion protein were affinity-purified using fusion protein coupled to activated CH-Sepharose 4B (Amersham Pharmacia Biotech). To block antiyeast antibodies in the rabbit anti-LexAp antiserum (Sassanfar and Roberts, 1990), the antiserum was mixed with an equal volume of yeast, fixed, zymolyase digested, methanol/acetone extracted as for immunofluorescence (Pringle et al., 1991), gently mixed overnight at 6°C, and centrifuged to remove cells and debris. Immunofluorescence was performed as described (Pruyne et al., 1998) using 1:50 anti-Myo2p and 1:100 anti-LexAp. To measure the proportion of cells containing polarized Sec4p and Myo2p, we identified a random small-budded cell by differential interference contrast (DIC), switched to viewing by fluorescence to score whether the bud or bud tip is brighter than the mother cell, then switched back to DIC and moved to a new field, repeating until we had scored 200, or in some experiments, 100 cells. For experiments where small-budded cells become scarce (75-min temperature shift of *myo2^{ts}* mutants or expression of LexA fusion protein) we counted all cells regardless of the cell cycle stage. Calcofluor staining (Pringle, 1991), vacuole inheritance (Hill et al., 1996), and endocytosis of the water-soluble dye Lucifer yellow (Dulic et al., 1991) were observed by the methods described. As negative controls, we tested DBY2000 (*act1-1*) and NY405 (*sec4-8*) for endocytosis: ~10 and 1%, respectively, take up Lucifer yellow at 37°C, compared with 50–75% of wild-type and *myo2^{ts}* cells.

Inducible Expression of Myo2p Fusion Proteins in Yeast

To express high levels of a GST fusion protein containing the Myo2p COOH-terminal region, pEGM was constructed by subcloning the EcoRI-ClaI fragment of pJP10-2B into pRS303, and then inserting the BglII-SalI fragment of the resulting plasmid into the BamHI and SalI sites of pEG, a 2μ plasmid with GST under *GAL* control (pEG[KG]) (Mitchell

1. *Abbreviations used in this paper:* GST, glutathione *S*-transferase; SD, synthetic minimal dextrose medium; YPD, yeast extract peptone-dextrose medium.

Table III. Myosin V Sequences Used

Organism	Protein name	Accession*	BLAST score for Myo2p globular tail, bits‡ (*P*)§		BLAST 2.0 score for core conserved region of tail‖, bits‡	
			BLAST 2.0	PSI-BLAST¶	Myo2p	Myo4p
Fungi						
Saccharomyces cerevisiae	Myo2p	sp | P19524	680		190	58
	Myo4p	sp | P32492	103 (10^{-20})		58	186
Schizosaccharomyces pombe	Myosin	emb | CAA22641	99 (10^{-19})		50	<23
	Myosin-2	emb | CAA21172	80 (10^{-13})		53	34
Animals						
Gallus gallus	Myosin-V, p190	pir | S19188	110 (10^{-23})		79	36
Homo sapiens	Myosin 12	emb | CAA69035	111 (10^{-23})		78	36
Mus musculus	dilute, Myosin 5a, Myosin H	sp | Q99104	112 (10^{-23})		78	36
	Myosin 5b	sp | P21271	92 (10^{-19})		73	37
Rattus norvegicus	myr6	gi | 1575333	99 (10^{-19})		73	38
Caenorhabditis elegans	hum-2	gi | 1279777	77 (10^{-12})		50	33
Drosophila melanogaster	Myosin V	gi | 4092802	69 (10^{-10})		52	<23
Plants						
Zea mays	Myosin XI	gb | AAD34597.1	51 (10^{-4})		41	25
	Myosin	gb | AAD17931.2		194 (10^{-48})	34	24
Helianthus annuus	Myosin	gi | 2444178	48 (10^{-4})		40	25
	Myosin	gi | 2444180		197 (10^{-49})	32	24
Arabidopsis thaliana	Myosin V, MYA1	pir | S46444	45 (10^{-3})	181 (10^{-44})	34	25
	MYA2	pir | S51824	49 (10^{-4})		37	24
	Myosin	gi | 3142302	46 (10^{-3})		36	<23
	Myosin	gi | 3776579		191 (10^{-47})	34	<23
	F22013.22	gi | 3063460		181 (10^{-44})	34	24
	Myosin	gb | AAD32282.1		162 (10^{-38})	36	23
	Myosin	gb | AAD21759.1		169 (10^{-40})	31	<23
	Myosin	emb | CAA22981.1		200 (10^{-50})	<23	<23
	Myosin	gi | 2924770		141 (10^{-32})	<23	<23
	Myosin	gi | 2494118		130 (10^{-28})	31	28
	Myosin	emb | CAB36794		99 (10^{-19})	26	25
Chlamydomonas reinhardtii	Myosin	gi | 3342148		157 (10^{-36})	<23	26
Slime mold						
Dictyostelium discoideum	Myosin IJ	sp | P54697		68 (10^{-10})	<23	<23

*All sequences obtained through the National Center for Biotechnology Information (http://www.ncbi.nlm.nih.gov).
‡Based on BLOSUM62 substitution matrix with a gap opening penalty of 11 units (~4.6 bits) and gap extension penalty of 1 unit (~0.4 bits).
§Where applicable. Scores $>10^{-3}$ not shown.
‖Residues 1389–1478 of Myo2p and residues 1307–1395 of Myo4p as shown in Fig. 8 C.
¶Single iteration using sequences with a BLAST 2.0 $P < 10^{-3}$ to construct the position-specific substitution matrix.

et al., 1993). A *CEN* plasmid, pCGM, was made by replacing the smaller NcoI-SalI fragment of pRS316 (Sikorski and Hieter, 1989) with the smaller NcoI-SalI fragment of pEGM. Similarly, pCG was made by replacing the smaller NcoI-XbaI fragment of pRS316 with the smaller NcoI-XbaI fragment of pEG. pCLM was made by replacing the SacI-NruI fragment of pCGM encoding GST with a PCR product encoding LexA protein plus one COOH-terminal glycine. This construct contains three silent mutations in LexA. pCL was constructed by cutting pCLM with ClaI, filling in the 5′ overhang, cutting with NruI, and recircularizing, thereby removing the entire *MYO2* sequence. Western blotting for GST and LexAp confirmed inducible expression of fusion proteins.

Sequence Analysis

A PSI-BLAST (Altschul et al., 1997) search for sequences significantly similar to the Myo2p tail identified 16 plant, 7 animal, 1 *Dictyostelium*, and 3 fungal myosin Vs (not including Myo2p). All have a conserved NH_2-terminal motor domain, six IQ repeats, a predicted coiled–coil region (COILS2) (Lupas, 1996), and the conserved tail domain (Table III), except for the mouse myosin Vb sequence, which is incomplete. Searching for sequences similar to the Myo4p tail failed to find additional myosins. Some authors (for example, Mooseker and Cheney, 1995) have grouped the plant and *Dictyostelium* myosins as a separate class, myosin XI. For the sake of clarity we call all of these myosins "myosin V," since they clearly form a distinct group with a common origin and since all of the experimentally characterized myosins of this group are called myosin V in the literature.

We used a parsimony method to determine the relationship among Myo2p, Myo4p, and *Schizosaccharomyces pombe* myosin V, using *Dictyostelium* myosin II as an outgroup. The three myosin V motor domains were independently aligned with myosin II, identifying 29 informative positions (where one residue occurs in two myosins and a different residue occurs in both of the other two myosins) in unambiguously aligned regions. These positions are widely dispersed in the motor domain structure and are spaced at least five residues apart.

CLUSTAL W (Thompson et al., 1994) provided an initial multiple alignment of amino acid sequences that was manually corrected by comparing with the outputs of BLAST and MEME (Bailey and Elkan, 1994) to find obvious alignment errors.

Other Methods

Western blotting and chemiluminescent protein detection was performed using a 1:2,000 dilution of affinity-purified anti-Myo2p antibody overnight at 6°C. Invertase accumulation was measured (Bankaitis et al., 1989) and cells tested for elevated specific gravity by mixing early log-phase cells with 92% Percoll (colloidal silica; Sigma Chemical Co.), then centrifuging at 12,000 *g* for 5 min. Wild-type cells float, whereas *sec6-4* and other *sec* mutants sink after incubation at the restrictive temperature.

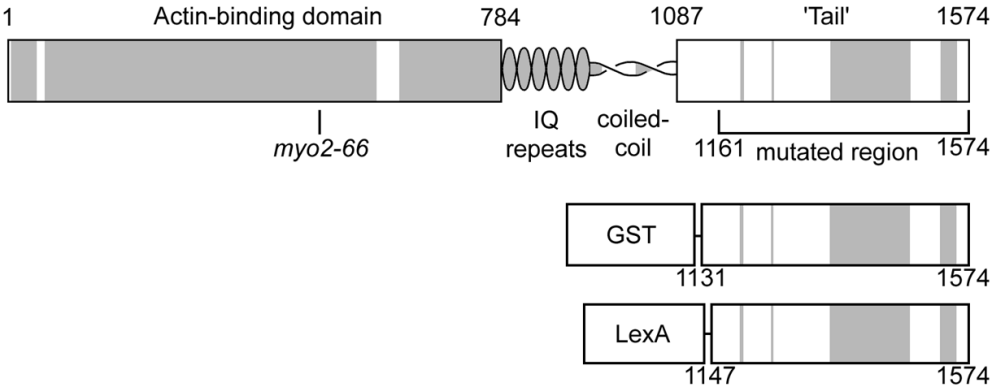

Figure 1. Myo2p. Predicted domain structure showing the region mutagenized and the fusion constructs used. Shaded regions are conserved between Myo2p and nonfungal myosin Vs.

Results

New Temperature-sensitive COOH-Terminal Domain myo2 Mutations

Much of the current knowledge about *MYO2* function comes from studies of the original *myo2* allele, *myo2-66* (Johnston et al., 1991), a mutation in the NH_2-terminal motor domain (Lillie and Brown, 1994). To investigate the COOH-terminal domain's function, we introduced random mutations into the chromosomal *MYO2* gene (Fig. 1) and screened for heat- and cold-sensitive mutants. We found seven new heat-sensitive alleles of *myo2* (Table IV) but no cold-sensitives. Temperature sensitivity is recessive in all *myo2^{ts}* tail mutants and none are complemented by

Table IV. myo2^{ts} Alleles

Allele	Predicted amino acid changes	Corresponding residue in other organisms*			Budded cells at 37°C 4 h	Diffuse chitin at 37°C 4 h	Vacuole inheritance at permissive temperature
		Animals	Plants	*Dicty.*‡			
					Y§	N§	Y‖
MYO2$^+$	Q1316L	I,L,V			N	Y	Y
myo2-12	H1373R	G	F,Y,N,H				
	Q1441L	Q	Q	E			
	D1457V	E,D	E,D	K			
	S1512T						
myo2-13	F1298Y	L		T	N	Y	Y
	Y1389C	I,F,W,M	F,Y				
	S1520G						
	D1543V						
myo2-14	Y1451D	K	P,Y	E	N	Y	Y
	G1461V	S,D,E	D,E	Q			
	L1536amber	¶					
myo2-16	M1212T				N	Y	Y
	L1471S	L,V	L	L			
	D1497V						
myo2-17	K1285R				N	Y	Y
	Y1287N						
	L1436S	L,M,F	L	F			
myo2-18	Y1161F				N	Y	Y
	N1171Y						
	L1413S	I,L	V	V			
	I1453V	D,E,P,H	K,I	I			
	I1498M						
myo2-20	E1168K				N	Y	Y
	N1254D	N	N				
myo2-66	E511K**	E	E	E	N‡‡	Y‡‡	N§§

*For unambiguously alignable residues.
‡*Dictyostelium discoideum.*
§Y, present in a large proportion of cells; N, rare or absent.
‖Y, >95% of small to medium-sized buds have inherited vacuole membrane; N, <5% of small to medium-sized buds have inherited vacuole membrane.
¶Four conserved residues in 23-residue COOH terminus.
**Lillie and Brown, 1994.
‡‡Also shown by Johnston et al., 1991.
§§Also shown by Catlett and Weisman, 1998.

myo2-66. All seven tail mutants have doubling times within ±15% of wild-type (95% confidence interval for each allele) in synthetic minimal medium (SD) at 24°C, showing that all are highly functional at the permissive temperature.

However, the growth rate of *myo2-12* yeast at 24°C is slowed if wild-type *MYO2* is introduced on a low-copy number plasmid, indicating a partial gain-of-function effect of this allele at permissive temperatures. The *myo2-12* mutation appears to make more drastic amino acid changes in Myo2p than any other *myo2^{ts}* tail mutation, replacing a polar residue and a charged residue, both conserved in nearly all myosin Vs, with hydrophobic residues (Table IV).

A phenotype common to *myo2-66* and most of the new *myo2^{ts}* alleles is sensitivity to rich media: rich media cause a 1–3°C reduction of the restrictive temperature (Table V) in all alleles except *myo2-14*. In addition, *myo2-12* and *myo2-16* mutants have slowed growth in rich media even at 24°C. The reason for this rich medium sensitivity is unclear; addition of filter-sterilized peptone (2%) strongly inhibits growth of *myo2-12* yeast (the most YPD-sensitive mutant) in SD, accounting for most of the inhibitory effect of rich media, whereas reduction of the glucose concentration partially restores growth to *myo2-12* yeast in YPD. Addition of 1 M sorbitol to provide osmotic support has no effect on *myo2-12* mutant growth in YPD.

Genetic Interactions of the New myo2^{ts} Alleles

To identify components that interact with the Myo2p tail, we screened for genes whose overexpression suppress *myo2-17*, *myo2-18*, or *myo2-20* temperature sensitivity. Our screen identified one clone of *SMY1*, a gene recovered previously as a multicopy suppressor of *myo2-66* (Lillie and Brown, 1992). Multicopy *SMY1* (YEpSMY1) dramatically suppresses *myo2-12*, *myo2-13*, *myo2-16*, *myo2-17*, and *myo2-18* temperature sensitivity and moderately suppresses *myo2-20*. Intriguingly, suppression of *myo2-66* in an isogenic strain is weaker than for the alleles mentioned above, and multicopy *SMY1* does not suppress *myo2-14* at all (Table V and data not shown).

The original *myo2-66* mutation is lethal in combination (synthetically lethal) with mutations in a broad spectrum of other genes, including a subset of genes affecting post-Golgi steps in secretion (Govindan et al., 1995). Since we are interested in the role of Myo2p in the polarized delivery of secretory vesicles, we wished to examine whether a *myo2^{ts}* tail mutation shows synthetic lethality with these mutations as well. We chose *myo2-13* because it is neither one of the most nor one of the least severe temperature-sensitive alleles we isolated. *myo2-13* is not synthetically lethal at 30°C on SD or YPD with *sec1-1*, *sec2-56*, *sec5-24*, *sec6-4*, or *sec9-4*. In contrast, *sec2-41*, *sec5-24*, and *sec9-4* have been reported to be synthetically lethal with *myo2-66* at 25°C (Govindan et al., 1995).

We also checked for synthetic lethality of all the new *myo2^{ts}* alleles with *sec4-8*. Like *myo2-66* (Govindan et al., 1995), *myo2-14* is synthetically lethal with *sec4-8*, whereas *myo2-12*, *myo2-13*, *myo2-16*, *myo2-17*, and *myo2-18* have only mild synthetic growth defects with *sec4-8* (Table V). Interestingly, *myo2-20* shows no synthetic growth defect at all with *sec4-8*.

Targeting of Secretory Vesicles to Growth Sites Requires the Myo2p Tail

Like *myo2-66* (Johnston et al., 1991), the new *myo2^{ts}* tail mutations block bud initiation and polarized growth at the restrictive temperature, with most of the cells arresting as very large, unbudded spheres (Table IV), indicating a block in polarized secretion even though secreted proteins still reach the cell surface. Furthermore, like *myo2-66* yeast, the new temperature-sensitive tail mutants deposit chitin diffusely over the cell surface at 37°C in SD (Table IV). In *myo2-66* yeast, this diffuse chitin distribution is due to a failure to target a membrane protein, the main chitin synthetase Chs3p, to the correct locations (Santos and Snyder, 1997).

To investigate whether loss of polarized secretion is a direct result of loss of Myo2p function, we looked at how rapidly the polarized distribution of Sec4p, a Rab GTPase component of late secretory vesicles (Mulholland et al., 1997; Walch-Solimena et al., 1997), disappears in *myo2^{ts}* mutants after shift to the restrictive temperature. In wild-type yeast, shifting to temperature above 35°C depolarizes actin, Myo2p, and Sec4p, which then return more than an hour later (Lillie and Brown, 1994). The polarized Sec4p

Table V. Genetic Interactions of myo2^{ts} Alleles

Allele	Restrictive temperature, rich media (minimal media)	Restrictive temperature in presence of high-copy *SMY1*, rich medium (minimal medium)	Restrictive temperature of *sec4-8* mutant, minimal medium
	°C	°C	°C
MYO2^{+}	>38 (>38)	ND	30
myo2-12	30 (33)	>36	27
myo2-13	35 (36)	>36	29
myo2-14	35 (35)	35 (35)	sl at 22
myo2-16	30 (33)	>36	27
myo2-17	35 (37)	>36	29
myo2-18	35 (37)	>36 (>37)	29
myo2-20	36 (37)	36 Semipermissive	30
myo2-66	27 (30)	30*	sl at 22‡

*Also shown by Lillie and Brown, 1992.
‡Also reported by Govindan et al. (1995) to be synthetic lethal at 25°C on YPD.
sl, synthetic lethal.

*Table VI. Effect of myo2 Mutations on Sec4p and Myo2p after 75-min Shift to 37°C**

Strain	Allele	Polarized Sec4p distribution, % of total cells	Polarized Myo2p distribution, % of total cells
ABY531	*MYO2*$^+$	46	28
ABY537	*myo2-17*	0	33
ABY538	*myo2-18*	0	38
ABY530	*myo2-20*	0	38

**myo2-12*, *myo2-13*, *myo2-14*, and *myo2-16* are not shown because Western blotting data indicate reduced levels of the mutant Myo2p after prolonged incubation at 37°C.

distribution fails to return in *myo2-66* (Lillie and Brown, 1994) and *myo2* tail mutants (Table VI).

To see the immediate effects of disrupting Myo2p function, we chose to look at *myo2-16* and *myo2-66* because their restrictive temperatures are low enough that shifting to these temperatures leaves the distribution of Myo2p, Sec4p, and the actin cytoskeleton relatively unaffected in wild-type yeast (Pruyne et al., 1998). In *myo2-16* yeast, the Sec4p distribution begins to depolarize within 1 min of temperature shift and is completely depolarized within 5 min (Fig. 2 A). In earlier studies, Walch-Solimena et al. (1997) showed that *myo2-66* blocks accumulation of Sec4p at growth sites after 1 h at 37°C, and Govindan et al. (1995) showed that *myo2-66* blocks the accumulation of secretory vesicles in small buds. Here we show that *myo2-66* yeast has a partially polarized distribution of Sec4p at 25°C that disappears very rapidly upon shift to a restrictive temperature (Fig. 2 A). The redistribution of Sec4p is complete within a 1-min shift to 30.5°C (data not shown). We conclude that the loss of Myo2p head or tail function depolarizes Sec4p, and presumably secretory vesicle targeting in <5 min.

Targeting of Myo2p to Growth Sites Requires a Functional Actin-binding Domain but Not a Functional COOH-Terminal Domain

Shifting *myo2-16* yeast to 35°C for 5 min, conditions that completely depolarize Sec4p, has no effect on the

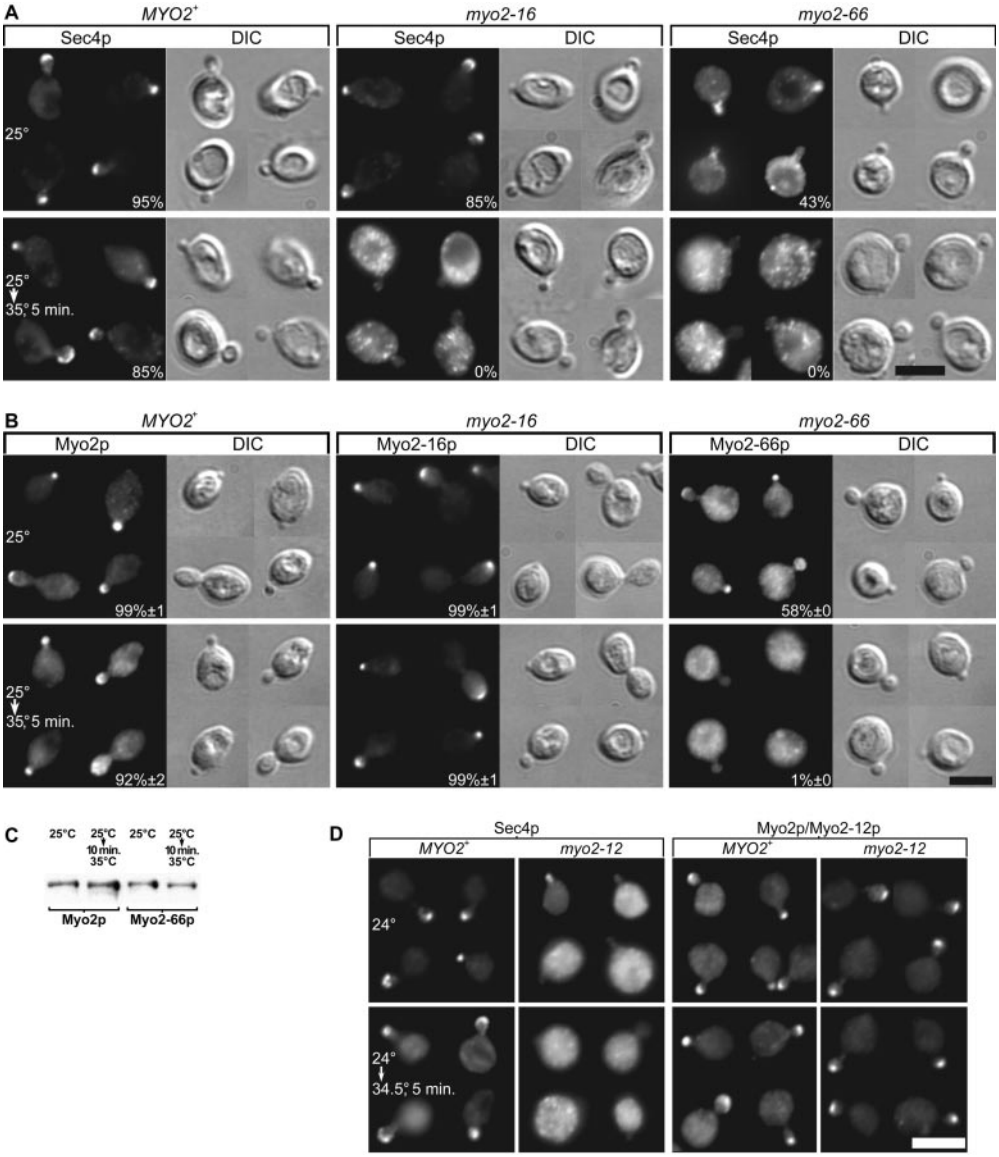

Figure 2. Effect of *myo2* mutations on the distribution of Sec4p and Myo2p. (A and B) ABY551 (*MYO2*$^+$), ABY553 (*myo2-16*), and ABY555 (*myo2-66*), grown in SD at 25°C, and shifted from 25 to 35°C for 5 min. (A) Sec4p staining, with percentages of small buds showing a polarized distribution. (B) Myo2p staining, with percentages ± SEM, $n = 2$ experiments. (C) Myo2-66p is not rapidly degraded at the restrictive temperature. Western blot of ABY551 and ABY555 lysates. (D) Sec4p and Myo2p staining of ABY531 (*MYO2*) and ABY532 (*myo2-12*). Bars, 5 μm.

Myo2-16p distribution (Fig. 2 B). *MYO2* wild-type yeast shows a slight depolarization of Myo2p upon shift to 35°C, such that Myo2-16p retains slightly greater polarity than wild-type Myo2p. Myo2-12p, another tail mutant, also remains polarized despite a depolarized Sec4p distribution (Fig. 2 D). Furthermore, Myo2-17p, Myo2-18p, and Myo2-20p are at least as polarized as wild-type Myo2p at 37°C (Table VI).

In contrast to Myo2-16p, the polarized distribution of Myo2-66p disappears very rapidly (within 5 min of shifting to 35°C) (Fig. 2 B), even though Myo2-66p is still present (Fig. 2 C). As is the case with Sec4p, the redistribution of Myo2-66p is nearly complete within 1 min shift to 30.5°C (data not shown), and even at the permissive temperature there is a substantial defect in Myo2-66p polarization (Fig. 2 B).

To test whether this polarized distribution of Myo2-16p reflects continued cable-dependent transport or simple trapping of the myosin at growth sites, the behavior of the tail mutant was examined in a background conditionally defective for cables (Pruyne et al., 1998). *tpm1-2 tpm2Δ myo2-16* cells shifted to 34.5°C lose cables as well as the polarized distribution of Myo2-16p (Fig. 3). When restored to a permissive temperature, cables reform and the mutant myosin repolarizes within 2 min, just as seen for wild-type myosin (*MYO2*$^+$ *tpm1-2 tpm2Δ* yeast) (Fig. 3 and Pruyne et al., 1998). Notably, Myo2-16p repolarizes despite the lack of Sec4p-associated cargo (Fig. 3). Again, a slightly greater proportion of *myo2-16* than *MYO2*$^+$ cells show a polarized Myo2p distribution.

The Myo2p Tail Is Not Directly Needed for Actin Cytoskeleton Polarity

myo2-16 has very little effect on the overall appearance of the actin cytoskeleton at 35°C. As seen by immunofluorescence, actin cables are as abundant as in wild-type yeast and remain aligned towards presumptive regions of growth (Fig. 4 A) even after prolonged incubation (1.5 h) at the restrictive temperature. Actin patches remain polarized at early timepoints (Fig. 4 A) and then slowly redistribute to an even distribution over the entire surface of the cell. Substantial depolarization of actin patches requires ~15 min of temperature shift and complete depolarization requires >30 min. At their restrictive temperatures, the other *myo2*^{ts} tail mutants show a similar actin distribution to *myo2-16*, except for *myo2-12* after prolonged incubation at a restrictive temperature, where a small proportion (≤1%) of cells contain actin bars similar to those seen in *myo2*-66 cells (Johnston et al., 1991). The bars presumably represent aberrant aggregates of unpolymerized actin, because antiactin antibody detects the bars whereas rhodamine-phalloidin, which binds actin filaments, does not.

The actin distribution in *myo2-66* yeast (Fig. 4 A) is remarkably similar to wild-type and *myo2-16*, except that even at the permissive temperature *myo2-66* yeast has subtle defects in the actin patch distribution. These results are consistent with the finding that functional Myo2p is unnecessary for the rapid assembly of actin cables (Pruyne et al. 1998). Actin bars are much less abundant (≤1% of

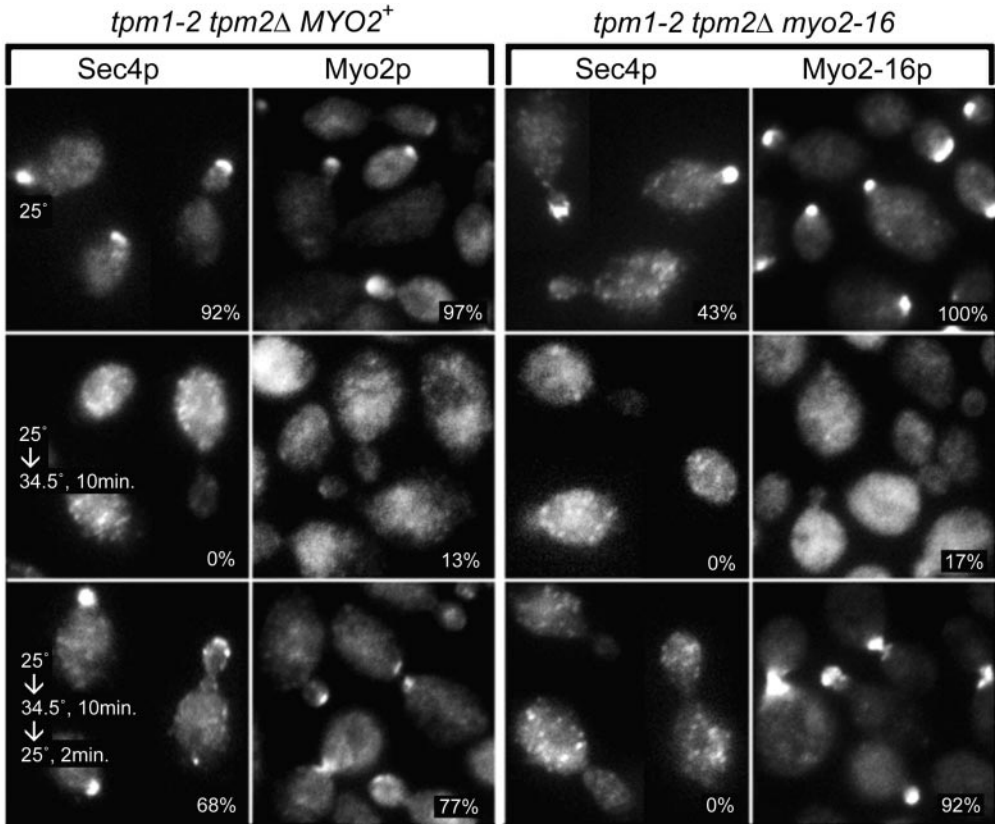

Figure 3. Myo2p and Sec4p distributions in *tpm1-2 tpm2Δ MYO2*$^+$ (ABY988) and *tpm1-2 tpm2Δ myo2-16* (ABY1128) yeast grown at 25°C (upper panels), shifted to 34.5°C for 10 min (middle panels), and then shifted back to 25°C for 2 min (lower panels). Percentages of small-budded cells showing a polarized distribution are shown.

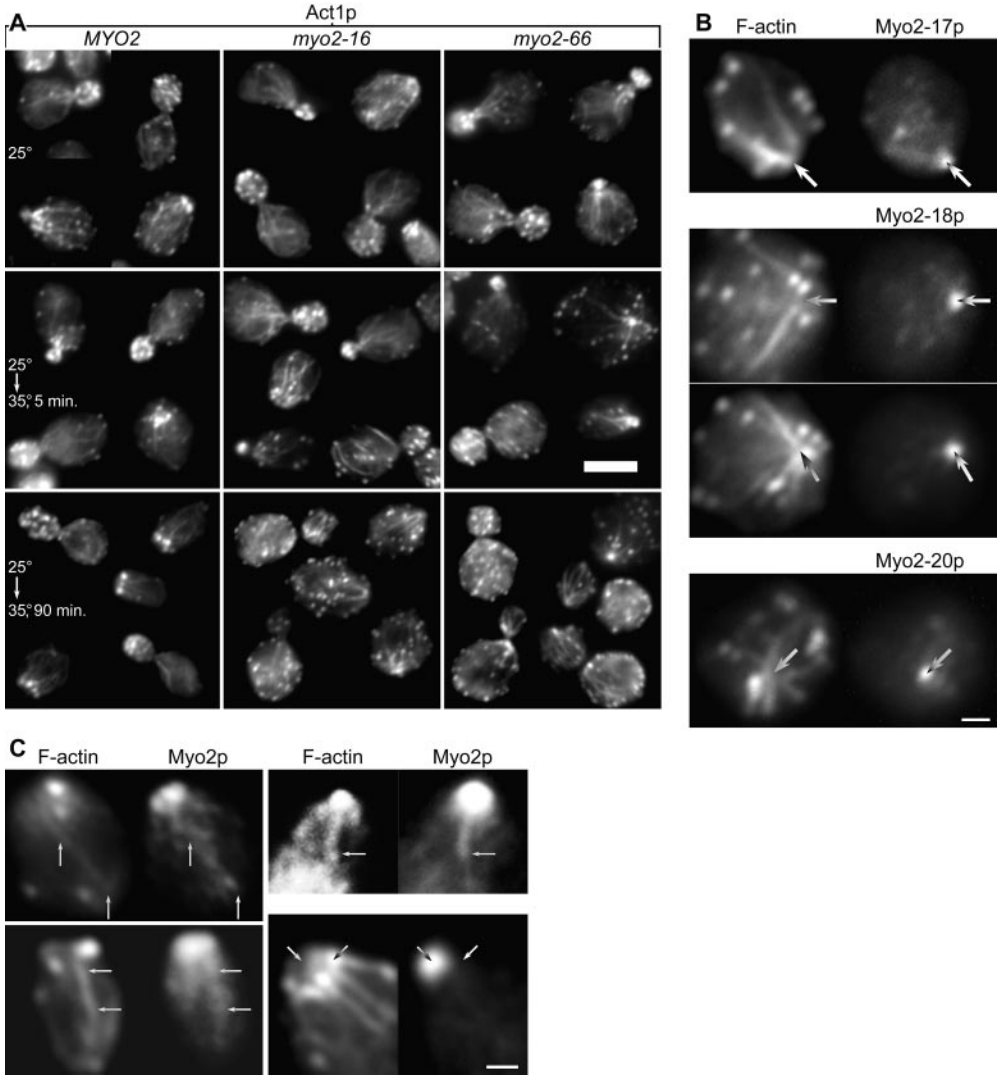

Figure 4. (A) Act1p (actin) immunofluorescence of ABY-551 (*MYO2*$^{+}$), ABY553 (*myo2-16*), and ABY555 (*myo2-66*) grown in SD at 25°C, shifted from 25 to 35°C for 5 min, or shifted for 90 min. Bar, 5 μm. (B and C) Yeast double-labeled for F-actin with rhodamine-phalloidin and for Myo2p. Bars, 1 μm. (B) Myo2p is concentrated where actin cables converge in ABY537 (*myo2-17*), ABY538 (*myo2-18*), and ABY530 (*myo2-20*), shifted to 37°C for 75 min. Images have been aligned using other cells in the same field and the faint cytoplasmic background in both fluorescence channels. Arrows mark the point of brightest Myo2p staining. (C) Gallery of selected wild-type cells in which the images have been overexposed to make faint structures more visible. Long arrows indicate faint structures that appear to contain both Myo2p and F-actin. Diagonal arrows in the lower right panel indicate bright Myo2p and F-actin structures that do not coincide.

cells) than reported by Johnston et al. (1991), a discrepancy probably accounted for by a difference in strain background and growth conditions.

If Myo2p moves along actin cables, it might partially colocalize with them. Indeed, in *myo2* tail mutants shifted for a long time to 37°C such that actin patches no longer obscure cables at polarized sites, the mutant Myo2p is concentrated at the point where cables converge (Fig. 4 B). Furthermore, Myo2p staining in wild-type yeast sometimes reveals faint cable-like structures and rows of Myo2p patches along actin cables (Fig. 4 C). This colocalization is not due to bleed-through between fluorescence channels, because the bright actin patches are not generally visible in the Myo2p images and the bright patch of Myo2p at the bud tip is not seen in the F-actin images (Fig. 4 C).

The myo2^{ts} Tail Mutations Have Little Effect on Vacuole Inheritance at Permissive Temperatures or Bulk Secretion and Endocytosis at Restrictive Temperatures

In addition to its role in polarized secretion, *MYO2* is also needed for polarized transport of the vacuole into the bud (Hill et al., 1996), and even at a permissive temperature, *myo2-66* blocks transfer of any part of the vacuole from the mother cell to the growing bud (Hill et al., 1996; this study) (Table IV). In addition, a screen for mutants defective in vacuole inheritance identified *myo2-2* (Catlett and Weisman, 1998), a Myo2p tail point mutation that does not dramatically affect polarized secretion (Catlett and Weisman, 1998). In contrast, none of the new *myo2^{ts}* mutants have any vacuole inheritance defect at 24°C (Table IV). Even at 34°C, a semipermissive temperature, 51% of *myo2-17* cells, 75% of *myo2-18* cells, and 64% of *myo2-20* cells show transfer of vacuole membrane to the bud, demonstrating only a partial defect (95% of wild-type cells transfer vacuoles to the bud).

A conditional mutant of actin shows a partial defect in invertase secretion (Novick and Botstein, 1985), but neither *myo2-66* (Johnston et al., 1991) nor the new *myo2* tail mutations shows a detectable defect in invertase secretion at the restrictive temperature (data not shown), showing that the *myo2* mutations disrupt polarized secretion without affecting fusion of invertase-containing secretory vesicles with the plasma membrane. The new *myo2* tail muta-

tions also fail to show the increase in specific gravity at the restrictive temperature seen in mutants blocking the secretory pathway (Novick et al., 1980).

Endocytosis requires many of the known components of the actin cytoskeleton (for review see Mulholland et al., 1999), but does not require a functional Myo2p motor domain (Govindan et al., 1995). After 20 min at 37°C, none of the new *myo2*^{ts} alleles affect endocytosis, assayed by uptake of Lucifer yellow, indicating that the Myo2p tail, like the motor, is dispensable for endocytosis.

Fusion Proteins Containing the Myo2p Tail Disrupt MYO2's Essential Function

We expressed fusion proteins containing the Myo2p COOH-terminal domain to see whether this domain would interfere with polarized delivery of secretory vesicles by competing with endogenous Myo2p. Expression of GST fused at the COOH terminus with residues 1131–1574 of Myo2p (Fig. 1) from a galactose-inducible promoter on either a multicopy plasmid (pEGM) (Fig. 5 A) or low-copy number plasmid (pCGM) completely blocks growth. Galactose concentrations of 0.02 and 0.08% are sufficient to block growth of cells bearing pEGM and pCGM, respectively, but expression of GST alone from either a high-copy (pEG) or low-copy (pCG) plasmid has no effect on growth at 2% galactose.

At high galactose concentrations (≥1%) >50% of the cells with pEGM or pCGM are lysed by 6 h of induction, but at lower concentrations (≤0.1%), cells with pEGM become spherical, very large, and mostly unbudded, like *myo2*^{ts} mutants. Also, like *myo2-66* yeast that has been shifted to the restrictive temperature for a long time (Johnston et al., 1991), a population of very tiny cells is also present, and presumably represent buds that have separated from the mother cell without growing to a normal size. Cells with pEGM and induced with 2% galactose show a normal polarized Sec4p distribution except at late timepoints, after 8 h in galactose, when most of the cells become inviable. 8 h is also the amount of time needed for full induction from the *GAL* promoter in the strains we use.

To confirm that the tail fusion protein is interfering with normal *MYO2* function rather than interfering with an unnatural target, we tested whether *myo2* mutants are hypersensitive to GST–Myo2p tail fusion protein by transforming isogenic *MYO2*$^{+}$ and *myo2*^{ts} strains with pEG and pEGM and testing growth on raffinose plates in the presence or absence of leucine. pEG and pEGM contain a partially defective *LEU2* allele, *leu2d*, which selects for two- to fourfold higher plasmid copy number in the absence of leucine than in the presence of leucine (Erhart and Hollenberg, 1983; Futcher and Cox, 1984), such that in the absence of leucine there is some expression from the *GAL* promoter despite the lack of galactose. Under these conditions, *MYO2*$^{+}$ yeast is unaffected by GST–Myo2p tail, but *myo2-12*, *myo2-14*, *myo2-16*, and *myo2-20* yeast grow poorly and become spherical and very large. Growth of *myo2-13* and *myo2-18* yeast is moderately slowed, whereas *myo2-17* yeast is only slightly affected (Fig. 5 B). We were unable to test *myo2-66* yeast because *myo2-66*, unlike the other *myo2* alleles, causes very poor growth at any temperature when raffinose is the sole carbon source, and we were unable to construct *myo2-66* strains capable of growing on nonfermentable media.

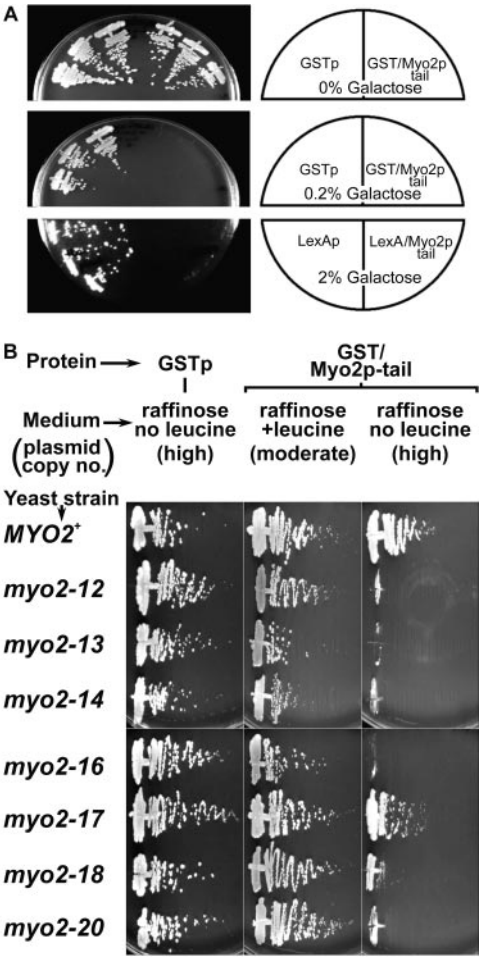

Figure 5. (A) Expression of Myo2p tail fusion protein is lethal. Three transformants each of ABY531 with pEG (GSTp), pEGM (GST–Myo2p tail), pCL (LexAp), or pCLM (LexA–Myo2p tail) were streaked onto raffinose or raffinose plus 0.2 or 2% galactose. (B) *myo2* tail mutants are hypersensitive to expression of tail fusion protein. ABY531 (*MYO2*), ABY532 (*myo2-12*), ABY533 (*myo2-13*), ABY534 (*myo2-14*), ABY536 (*myo2-16*), ABY537 (*myo2-17*), ABY538 (*myo2-18*), and ABY530 (*myo2-20*) bearing pEGM (GST–Myo2p tail) or pEG (GSTp) were streaked onto raffinose medium containing or lacking leucine and incubated at 30°C. Media lacking leucine select for cells with high plasmid copy number. Results are identical for at least four independent transformants for each combination of strain and plasmid.

Myo2p Tail Fusion Protein Is Concentrated at Growth Sites by Myo2p-targeted Secretory Vesicles

To see the subcellular distribution of Myo2p tail fusion protein, we tagged residues 1147–1574 of Myo2p with LexAp, a bacterial protein (Fig. 1). Expression of LexA–Myo2p tail fusion protein from a *GAL* promoter on a low-copy number plasmid (pCLM) is lethal (Fig. 5 A). Immunofluorescence shows that 1–2 h after addition of 2% galactose, 10–40% of cells (depending on strain background)

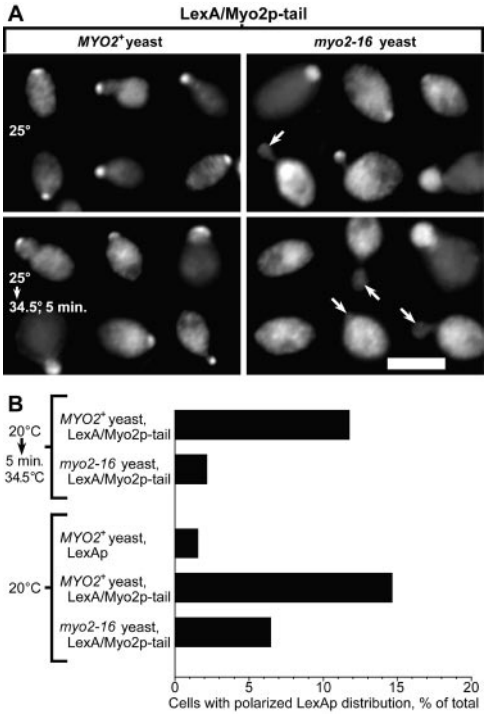

Figure 6. The polarized distribution of LexA–Myo2p tail requires functional endogenous *MYO2*. (A) Immunofluorescence of LexA in ABY551 (*MYO2*) and ABY553 (*myo2-16*) bearing pCLM, grown in raffinose medium with 2% galactose added for 60 min at 25°C, then shifted to 34.5°C for 5 min. Arrows indicate small buds lacking LexA staining. Images overrepresent the proportion of polarized cells severalfold. Bar, 5 μm. (B) Percentages of cells showing polarized LexA staining. ABY551 ($MYO2^+$) and ABY553 (*myo2-16*) bearing pCLM or pCL were grown in raffinose medium, then supplemented with 2% galactose for 90 min at 20°C or for 85 min at 20°C, then 34.5°C for 5 min. For each condition, 200 random cells in four separate trials were scored for staining concentrated at presumptive growth sites. After shift to 34.5°C, *myo2-16* cells are less often polarized for LexAp staining than wild-type ($P \leq 0.05$, two-tailed *t* test).

transformed with pCLM show a polarized distribution of LexAp similar to the polarized distribution of Sec4p and Myo2p (Fig. 6). Sec4p and the endogenous Myo2p distribution (using an antibody raised to a region outside the tail) is normal in these cells. With longer induction times (>4 h in galactose) the distribution of LexA–Myo2p tail in cells bearing pCLM becomes depolarized. Some of the larger-budded cells (1–9% at 1–2 h induction, rising to 20% at 4 h) show depolarized LexA–Myo2p tail and bright lumps of staining near the bud neck. Cells expressing LexAp alone (bearing pCL) show diffuse cytoplasmic staining, with a small proportion of cells that also show bright lumps of staining randomly distributed in the cell (data not shown). The clumping seen in both these cases might represent aggregation in those cells that express high levels of protein, since LexAp multimerizes at high concentrations (Schnarr et al., 1985), but notably, only the Myo2p tail fusion protein polarizes within the cell.

To test whether this polarized distribution of LexA–Myo2p tail fusion protein depends on polarized targeting of secretory vesicles, we looked at the distribution of LexA–Myo2p tail fusion protein in a *myo2-16* mutant. After 5 min shift to 34.5°C, *myo2-16* yeast shows a greatly reduced number of cells with polarized LexA–Myo2p tail protein compared with $MYO2^+$ yeast (Fig. 6). The distribution of endogenous Myo2-16p is normal in the *myo2-16* cells.

These results indicate that the polarized distribution of the Myo2p tail fusion protein requires an endogenous Myo2p motor protein with a functional tail domain. This could be because either the tail fusion protein binds directly to full-length Myo2p and this site is defective in *myo2-16*, or the tail fusion protein binds to secretory vesicles normally transported by full-length Myo2p. To distinguish between these two possibilities, we examined whether the fusion protein becomes depolarized in a *sec2-41* mutant. Walch-Solimena et al. (1997) have shown that Sec4p becomes depolarized in *sec2* cells after 10-min shift to 37°C, indicating that polarized delivery of secretory vesicles requires Sec2p, the nucleotide exchange factor for Sec4p. The polarized distribution of LexA–Myo2p tail is reduced in *sec2-41* yeast after 5-min shift to 35°C (Fig. 7, A and B). The polarized distribution of Sec4p also disappears, showing that secretion is no longer polarized. However, the distribution of endogenous full-length Myo2p is normal in the *sec2-41* cells, showing that the mechanism whereby *sec2-41* disrupts Sec4p and LexA–Myo2p tail targeting does not involve disrupting the targeting of full-length Myo2p. In contrast, *sec1-1*, which blocks vesicle fusion but not targeting, increases the frequency of polarized LexA–Myo2p tail distribution upon temperature shift (Fig. 7, A and B).

The Myo2p and Myo4p Tail Sequences Reflect Their Divergent Functions

The two myosin V genes of yeast, *MYO2*, required for polarized membrane transport, and *MYO4*, required for polarized mRNA targeting (Long et al., 1997; Takizawa et al., 1997), afford an opportunity to find protein sequences specifically involved in membrane binding. *Saccharomyces* has undergone a genome duplication sometime after it diverged from another Ascomycete, *Kluyveromyces* (Wolfe and Shields, 1997), and *MYO2* and *MYO4* lie in an unambiguously duplicated region (Fig. 8 A) (Parle-McDermott et al., 1996; Pearson et al., 1996; Storms et al., 1997). In support of a recent duplication, the Myo2p and Myo4p tails are more similar to each other than to any other myosin V. Furthermore, phylogenetic analysis of motor domain sequences (Fig. 8 B) shows that Myo2p and Myo4p diverged from each other after they diverged from a *Schizosaccharomyces pombe* myosin V, the most similar known protein to Myo2p and Myo4p.

Despite this evidence for a relatively recent origin of two different myosin Vs in yeast, animal myosin Vs are much more similar to Myo2p than to Myo4p in the COOH-terminal half of the tail. Fig. 8 C shows the two extensive regions that can be unambiguously aligned among animal myosin V tails and both Myo2p and Myo4p (matches highlighted in blue). Chicken p190, a biochemically well-characterized myosin V (Cheney et al., 1993), is shown as an example of an animal myosin V. Strikingly, in

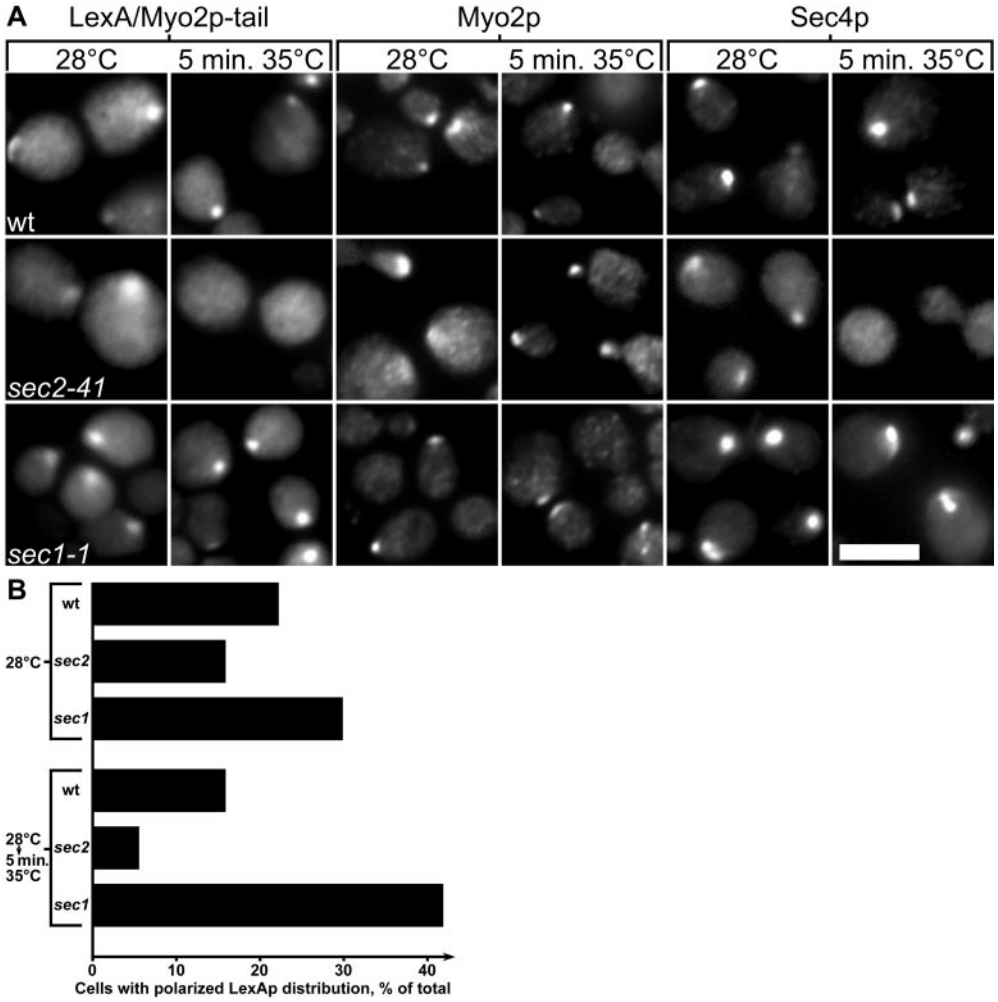

Figure 7. The polarized distribution of LexA–Myo2p tail requires functional *SEC2*. (A) LexAp, Myo2p, and Sec4p in NY13 (wt, upper panels), NY130 (*sec2-41*, middle panels), and NY3 (*sec1-1*, lower panels) bearing pCLM, grown in raffinose, then supplemented with 2% galactose for 60 min at 28°C and then shifted to 35°C for 5 min. Bar, 5 μm. (B) Percentages of cells showing polarized LexAp staining. After shift to 35°C, *sec2-41* cells are less often polarized for LexAp staining than wild-type ($P \leq 0.05$, two-tailed *t* test), whereas *sec1-1* cells are more often polarized for LexAp staining than wild-type ($P \leq 0.05$).

both regions animal myosin Vs are much more similar to Myo2p than to Myo4p (Fig. 8 C, red boxes). Plant myosin Vs (also known as myosin XIs) show less similarity to yeast myosin Vs, but nevertheless tend to be more similar to Myo2p than to Myo4p in this region (Table III and Fig. 8 C, green boxes). Since the animal myosin Vs are known to transport membranes (Mermall et al., 1998), the simplest interpretation is that the distal half of the Myo4p tail has lost features involved in membrane transport which are conserved in Myo2p and animal myosin Vs. Notably, most of the *myo2*^{ts} tail mutations make at least one nonconservative change in this region, and changes in the more distal regions correlate with *sec4-8* synthetic growth defects (Fig. 8 D).

Discussion

Since the original description of the *myo2-66* mutation's effect on polarized secretion (Johnston et al., 1991), Myo2p's precise role has been elusive. Models for Myo2p function have proposed that the motor transports secretory vesicles tethered to the COOH-terminal globular domain down tropomyosin-containing actin cables to their site of exocytosis (Johnston et al., 1991; Pruyne et al., 1998), or alternatively, that the COOH-terminal domain binds the plasma membrane at polarized sites, which indirectly leads to targeting of secretory vesicles to growth sites (Reck-Peterson et al., 1999), possibly by polarizing the actin cytoskeleton (Lillie and Brown, 1998). To distinguish between these models and to shed more light on the role of Myo2p, we have characterized new conditional alleles of *myo2* with defects in the COOH-terminal domain. Our results provide strong support for a model in which Myo2p binds secretory vesicles through its COOH-terminal domain and transports them down actin cables to regions of cell growth.

The Myo2p COOH-Terminal Globular Domain Carries Vesicular Cargo

We show that polarized secretion requires a functional Myo2p COOH-terminal globular domain: the tail mutants show depolarized growth, isotropic chitin deposition and loss of bud emergence, like the original motor mutant. These results are the first to directly implicate the Myo2p tail in polarized delivery of secretory vesicles.

Loss of the secretory vesicle component Sec4p from polarized sites occurs within 5 min of shifting the tail mutant *myo2-16* to the restrictive temperature. By contrast, both Myo2-16p and the actin cytoskeleton remain polarized for

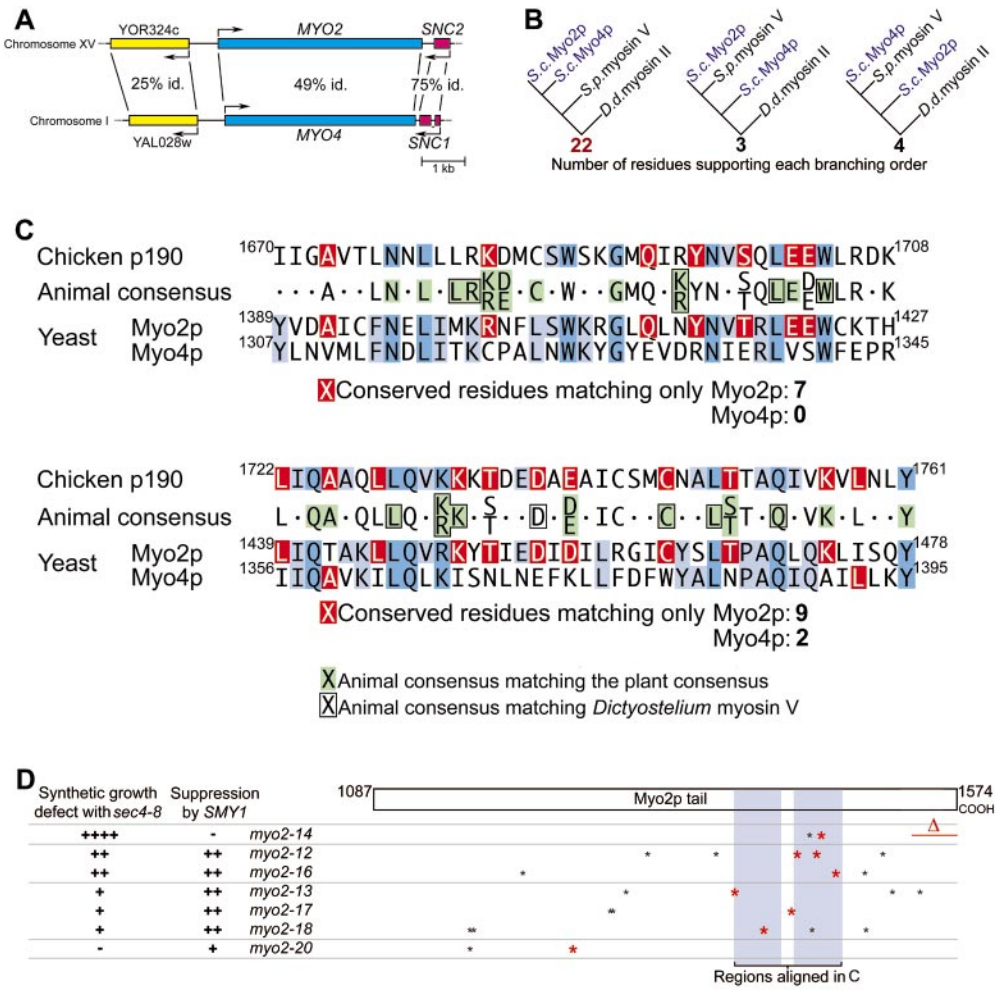

Figure 8. Myo2p has features conserved with animal myosin Vs but lost from Myo4p. (A) Map of genomic regions near *MYO2* and *MYO4*. Percentage of amino acid identity is shown ($P \leq 10^{-21}$ for all three BLASTP 2.0 scores). (B) Evolutionary relationship among the motor domains of Myo2p, Myo4p, and their closest relative, *Schizosaccharomyces* myosin V (CAA22641), using *Dictyostelium* myosin II as an outgroup. 22/29 corresponds to $P(\chi^2) \leq 10^{-6}$ and a bootstrap value of 99.7%. (C) Comparison of unambiguously alignable regions of p190, Myo2p, and Myo4p, showing consensus sequence for animal myosinVs, and matches of the animal consensus with the plant consensus (green) and *Dictyostelium* myosin V (boxed) sequences. Residues in the consensus sequence matching only Myo2p or only Myo4p are shown in red and other matches among the sequences are shown in blue. The animal consensus represents residues that match in at least six of the seven animal myosin Vs. (D) Summary of genetic interactions and positions of *myo2*^{ts} mutations relative to the regions aligned in C. Nonconservative mutations in residues that are conserved with animals are shown in red.

>15 min, demonstrating that the redistribution of Sec4p in *myo2-16* mutants is not due to Myo2p mistargeting or actin cytoskeleton depolarization. Since the Sec4p and Myo2p distributions are normally identical but temperature-shifting *myo2-16* yeast disrupts only the Sec4p distribution, the simplest interpretation is that the tail tethers vesicles to Myo2p.

Additional evidence that the tail binds secretory vesicle cargo comes from yeast expressing fusion proteins containing the Myo2p tail. Isotropic growth and loss of bud emergence, the same phenotypes as *myo2*^{ts} mutants, combined with the hypersensitivity of *myo2* tail mutants to tail fusion protein, show that tail fusion proteins disrupt Myo2p's normal function in polarized secretion. These fusion proteins presumably compete with the endogenous Myo2p tail for a factor in limited supply, such as a receptor for Myo2p on secretory vesicles. Accordingly, fusion protein initially concentrates at the same polarized sites as Myo2p and Sec4p. As we describe below, this initial distribution probably represents fusion protein bound to secretory vesicles, which are carried by endogenous Myo2p to growth sites, before fusion protein expression reaches saturating levels.

While this study was in the final stages of assembly, Reck-Peterson et al. (1999) reported a similar approach with an epitope-tagged Myo2p tail construct that, like our constructs, lethally disrupts polarized secretion and initially concentrates at polarized sites. Although Reck-Peterson et al. (1999) concluded that the Myo2p tail localizes independently of the rest of the molecule, we found no evidence to support that conclusion. Instead, we found that the polarized distribution of tail fusion protein depends on functional full-length Myo2p, as demonstrated in a *myo2-16* mutant shifted to the restrictive temperature.

More specifically, polarized secretion is essential for a polarized tail fusion protein distribution. The *sec2-41* mutation disrupts the targeting of secretory vesicles to growth sites (Walch-Solimena et al., 1997). Shifting *sec2-41* yeast

to the restrictive temperature for 5 min also disrupts the tail fusion protein's polarized distribution, even though endogenous Myo2p stays at growth sites, showing the tail fusion protein does not bind to endogenous Myo2p directly but probably binds to its cargo instead. Furthermore, since *sec1-1* blocks vesicle fusion with the plasma membrane but not vesicle targeting, resulting in an initial hyperaccumulation of vesicles at growth sites (Govindan et al., 1995; Walch-Solimena et al., 1997), the increased frequency of polarized tail fusion protein in *sec1-1* yeast shifted to the restrictive temperature also suggests that the tail fusion protein resides on secretory vesicles.

Catlett and Weisman (1998) recently proposed direct binding of the vacuole to the Myo2p tail and describe *myo2-2*, a tail mutant that blocks vacuole transport with relatively little effect on polarized growth, in contrast to the tail mutant *myo2-12* described here, which has no effect on vacuole transport at a temperature where the Sec4p distribution is highly defective (Fig. 2 D) and growth is sensitive to rich media. For comparison, *myo2-66* completely blocks vacuole inheritance at permissive temperatures. These combinations of phenotypes are difficult to reconcile with simple models that do not involve binding of the tail to specific cargo membranes.

In light of Myo2p's role in secretory vesicle transport, the rich medium sensitivity of *myo2* mutants might be related to the rich medium sensitivity reported for *sec3* (Haarer et al., 1996) and *snc1Δ snc2Δ* mutants (Protopopov et al., 1993). *SEC3* and the two *SNC* synaptobrevin genes are needed for efficient fusion of secretory vesicles with the plasma membrane (Novick et al., 1980; Protopopov et al., 1993), but are not absolutely essential. Since nutrient compositions that speed the growth of wild-type yeast slow the growth of most $myo2^{ts}$ mutants, it is plausible that the increased production of secretory vesicles in rich media exceeds the mutant Myo2p's capacity to transport vesicles, leading to vesicle fusion at inappropriate sites in addition to the appropriate sites. Mistargeted secretion might be harmful if secretory vesicles carry a spatial signal that normally helps maintain cell polarity. Given the polarized distribution of parts of the vesicle docking and fusion machinery, including Sec3p (Finger et al., 1998), the same principle might apply to *sec3* and *snc1Δ snc2Δ* mutants, where increased vesicle production in rich media could swamp the capacity of polarized fusion sites leading to fusion at inappropriate sites.

The Myo2p NH_2-Terminal Actin-binding Domain Targets Myo2p to Growth Sites

The *myo2-66* mutation removes a salt bridge in a conserved actin-binding loop of the Myo2p NH_2-terminal motor domain (Lillie and Brown, 1994). Lillie and Brown (1994) have shown the loss of Myo2-66p localization in a *myo2-66* mutant shifted to 32°C for 75 min, whereas Walch-Solimena et al. (1997) have shown the loss of Sec4p localization in a *myo2-66* mutant shifted to 37°C for 1 h. Here we show that the depolarization of Myo2-66p and Sec4p in *myo2-66* yeast is extremely rapid, indicating that the motor domain is directly responsible for targeting Myo2p to the correct parts of the cell.

Conversely, temperature shifting *myo2-16*, a tail mutant, does not depolarize the Myo2-16p distribution, even though it completely depolarizes Sec4p. Instead, the Myo2-16p distribution is slightly more polarized than in wild-type yeast, which might be expected if Myo2-16p is released from vesicles that otherwise sterically slow down access of Myo2p to actin cables. The retention of Myo2-16p's polarized distribution reflects active cable-dependent transport rather than trapping of Myo2-16p at the growth site, as the loss of cables in *myo2-16 tpm1-2 tpm2Δ* yeast depolarizes Myo2-16p but the restoration of cables rapidly repolarizes Myo2-16p.

How, then, do we account for the Ayscough et al. (1997) finding that some Myo2p still concentrates at polarized sites despite depolymerization of actin with latrunculin-A? Growth sites may nucleate or stabilize actin filaments so strongly that actin filaments remain there, but are too short or sparse to be detectable by fluorescence microscopy. Alternatively, parts of the vesicle docking machinery may remain at polarized sites such that Myo2p can bind there. For example, latrunculin-A has no effect on the polarized distribution of Sec3p, a protein required for efficient vesicle fusion or docking (Finger et al., 1998). However, this is unlikely to be the normal mechanism for Myo2p localization, as actin cable–dependent targeting of Myo2p is much more rapid and robust. Our attempts at reproducing the polarized Myo2p distribution in the presence of latrunculin-A have failed: all of the treated cells have a diffuse Myo2p distribution, even the few cells that still have cortical actin patches faintly visible by rhodamine-phalloidin staining, whereas untreated cells have a normal Myo2p distribution.

We also need to account for the depolarized Myo2p distribution that has been reported for cells with disrupted Myo2p tail function, namely cells expressing the Myo2p tail construct of Reck-Peterson et al. (1999) and cells with the tail mutation *myo2-2* that Catlett and Weisman (1998) isolated on the basis of a vacuole inheritance defect. The simplest explanation is that the Myo2p distribution represents a balance between rapid translocation of Myo2p along cables to growth sites, and slower release or diffusion from those sites. The tail construct and *myo2-2* may disrupt interactions that would otherwise retain Myo2p at growth sites or slow Myo2p diffusion. Since the Myo2p tail construct used by Reck-Peterson et al. (1999) contains an additional 44-residue segment (residues 1087–1130) and the single amino acid change in *myo2-2* is at residue 1248, another explanation is that the relatively unconserved proximal region of the tail might regulate Myo2p's motor activity and translocation to the growth site. A precedent for autoregulation of a myosin by its COOH-terminal tail comes from a nonmuscle myosin II and a myosin I whose tails inhibit Mg^{2+}-ATPase activity (Citi and Kendrick-Jones, 1987; Stoffler and Bahler, 1998).

Nevertheless, cargo does not seem to regulate Myo2p motor activity very strongly if at all, given the normal intracellular distribution of Myo2p in the absence of bound secretory vesicle cargo. Note that our results show that Myo2p continually cycles into the bud whether or not secretory vesicles are present. Indeed, the Myo2p distribution is unaffected by *sec12-4*, which blocks the production of secretory vesicles at the restrictive temperature (data not shown).

Myo2p Is Not Directly Involved in Organizing the Actin Cytoskeleton

We show that the formation and polarity of actin patches and cables do not directly require functional *MYO2*. Specifically, the actin cytoskeleton is unaffected in *myo2^{ts}* mutants in the first minutes after shift to the restrictive temperature during which secretion becomes delocalized. However, cortical patches do eventually depolarize after 15–30 min of loss of either Myo2p protein function or tropomyosin-containing actin cables (Pruyne et al., 1998). In contrast, actin patches depolarize within 1 min in wild-type yeast in response to stresses such as heat shock (Lillie and Brown, 1994; data not shown) and centrifugation (Pringle et al., 1991), indicating that the effect of Myo2p and tropomyosin on actin patches is indirect.

The Distal Half of the Myosin V COOH-Terminal Globular Domain Contains Features Associated with Vesicle Transport

Among those post-Golgi secretory mutants that are synthetically lethal with *myo2*-66, the small Rab GTPase mutant *sec4-8* is particularly interesting, because Sec2p, its guanine nucleotide exchange factor, is the only *SEC* gene product known to be needed for polarized vesicle delivery (Walch-Solimena et al., 1997), suggesting that Sec4p marks vesicles for targeting to growth sites. We have found that a *sec2* mutation rapidly depolarizes secretion at the restrictive temperature without affecting the Myo2p distribution (Fig. 7 A), indicating that the *sec2* mutation uncouples secretory vesicles from Myo2p. Furthermore, Sec4p resides specifically on the surface of late secretory vesicles in wild-type yeast (Mulholland et al., 1997; Walch-Solimena et al., 1997), and of the late *sec* mutations, *sec4-8* and *sec2-41* are the only ones known to be synthetically lethal with *Δsmy1* (Lillie and Brown, 1998), implying a relatively direct interaction with *MYO2*. The new *myo2^{ts}* alleles provide additional insight into these interactions.

Of the COOH-terminal *myo2^{ts}* alleles, *myo2-14* is by far the most deleterious in combination with *sec4-8*. The trivial explanation, that *myo2-14* is the most severe allele below 30°C, is unlikely; both *myo2-12* and *myo2-16* have milder synthetic growth defects with *sec4-8*, but have lower restrictive temperatures than *myo2-14* and impair growth in rich media, even at 24°C. The region altered in *myo2-14*, the COOH-terminal 123 residues (Table IV and Fig. 8 D), is therefore likely to be important for Sec4p- and Sec2p-dependent vesicle targeting. This strong allele specificity and the uncoupling of secretory vesicles from Myo2p in a *sec2-41* mutant support a model in which a vesicle-associated Rab protein and its guanine nucleotide exchange factor direct vesicle transport either by physically tethering the myosin V COOH terminus to vesicles or by activating a latent myosin V COOH terminus–binding receptor on the vesicle surface.

A screen for multicopy suppressors of *myo2^{ts}* tail mutants identified *SMY1*, which has been isolated previously as a suppressor of *myo2-66* (Lillie and Brown, 1992). *SMY1* encodes a kinesin homologue that, like Myo2p, concentrates in regions of growth (Lillie and Brown, 1994) and aids *MYO2* function by a mechanism involving neither a kinesin-like motor activity nor microtubules (Lillie and Brown, 1998).

Since *myo2-14* is the only *myo2^{ts}* mutant whose growth is unaltered by multicopy *SMY1*, some part of the COOH-terminal 123 residues of Myo2p must affect functional interaction with *SMY1* in addition to *SEC4*, most likely the final 30 residues because *myo2-14* is the only allele that changes this part of the extreme COOH terminus (Fig. 8 D). It is unlikely that suppression of *myo2-14* by *SMY1* was overlooked due to a narrow temperature range where *myo2-14* is only partially functional, as *sec4-8* lowers *myo2-14*'s restrictive temperature by at least 13°C. The strong suppression of some but not all COOH-terminal globular domain mutants by multicopy *SMY1*, but comparatively weak suppression of the motor domain mutant, taken together with Smy1p's and Myo2p's identical subcellular distributions (Lillie and Brown, 1994), and Smy1p's apparent lack of its own motor activity (Lillie and Brown, 1998), suggests that Smy1p binds to the Myo2p globular tail domain directly. Binding of a kinesin to a myosin V tail has been demonstrated in an animal system (Huang et al., 1999), consistent with organelle transport occurring along microtubules using kinesin motors and then switching to myosin-driven transport along actin filaments near the final delivery site. Binding of a kinesin homologue to the Myo2p tail could have originated in yeast's hyphal ancestors. If so, Smy1p would have been kept because it stabilizes a multiprotein complex with the Myo2p tail needed for docking onto organelles, but Smy1p's microtubule-binding and motor activities would have been lost in a cell too small and compact to need microtubule-based vesicle transport.

Finally, comparison of the Myo2p sequence and the sequence of Myo4p, an RNA-transporting myosin V in yeast, with type V myosins in other organisms supports a model in which, after duplication of the yeast genome (Wolfe and Shields, 1997) resulting in two myosin V genes, one yeast myosin V selectively retained and the other yeast myosin V selectively lost features needed for membrane transport. These features are concentrated in the final 183 amino acid residues of Myo2p, a region that also contains the tail sequences most conserved among fungi, plants, animals, and cellular slime molds. In particular, animal myosin Vs known to be involved in membrane transport are much more similar in tail sequence to Myo2p than to Myo4p, despite overwhelming evidence that *MYO2* and *MYO4* arose from a comparatively recent duplication. Most of the tail mutations we isolated that affect polarized secretion make at least one nonconservative change in this region (Fig. 8 D). Nevertheless, the varying effects of tail mutations on vesicle transport compared with vacuole transport implies that the recognition of different organelles involves different features of the myosin tail.

On the other hand, plant and *Dictyostelium* myosin V tails are more similar to Myo4p than to Myo2p in a more proximal part of the tail (data not shown), but the functions of these myosin Vs are unknown. It would be interesting to know whether these myosins transport RNA, membranes, or both.

In summary, the data presented here support a model for polarized secretion in which a myosin V COOH-terminal globular domain binds vesicles, and the NH_2-terminal

motor domain drives translocation of the myosin and its attached cargo along tropomyosin-containing actin cables to the cargo's destination. This cycle of myosin V transport does not depend on the secretory cargo marked by Sec4p, and we have identified regions of Myo2p tail that might bind cargo.

We are grateful to the countless people who generously shared strains, plasmids, and reagents, and in particular to Peter Novick and Ruth Collins for providing anti-Sec4p antibody.

D. Schott was supported by the Spencer T. and Ann W. Olin Foundation (not to be confused with the other Olin Foundation) through Cornell University during part of this study. This work was supported by National Institutes of Health grant GM39066.

Submitted: 2 August 1999
Revised: 7 October 1999
Accepted: 14 October 1999

References

Adams, A.E.M., and J.R. Pringle. 1984. Relationship of actin and tubulin distribution to bud growth in wild-type and morphogenetic-mutant *Saccharomyces cerevisiae*. *J. Cell Biol.* 98:934–945.

Altschul, S.F., T.M. Madden, A.A. Schäffer, J. Zhang, Z. Zhang, W. Miller, and D.J. Lipman. 1997. Gapped BLAST and PSI-BLAST: a new generation of protein database search programs. *Nucleic Acids Res.* 25:3389–3402.

Ausubel, F.M., R. Brent, R.E. Kingston, D.D. Moore, J.G. Seidman, J.A. Smith, and K. Struhl, editors. 1996. Current Protocols in Molecular Biology. John Wiley & Sons, Inc., New York. 1,906 pp.

Ayscough, K.R., J. Stryker, N. Pokala, M. Sanders, P. Crews, and D.G. Drubin. 1997. High rates of actin filament turnover in budding yeast and roles for actin in establishment and maintenance of cell polarity revealed using the actin inhibitor latrunculin-A. *J. Cell Biol.* 137:399–416.

Bailey, T., and C. Elkan. 1994. Fitting a mixture model by expectation maximization to discover motifs in biopolymers. Proceedings of the Second International Conference on Intelligent Systems for Molecular Biology. AAAI Press, Menlo Park, CA. 28–36.

Bankaitis, V.A., D.E. Malehorn, S.D. Emr, and R. Greene. 1989. The *Saccharomyces cerevisiae SEC14* gene encodes a cytosolic factor that is required for transport of secretory proteins from the yeast Golgi complex. *J. Cell Biol.* 108:1271–1281.

Cadwell, R.C., and G.F. Joyce. 1992. Randomization of genes by PCR mutagenesis. *PCR Methods Appl.* 2:28–33.

Catlett, N.L., and L.S. Weisman. 1998. The terminal tail region of a yeast myosin-V mediates its attachment to vacuole membranes and sites of polarized growth. *Proc. Natl. Acad. Sci. USA*. 95:14799–14804.

Cheney, R.E., M.K. O'Shea, J.E. Heuser, M.V. Coelho, J.S. Wolenski, E.M. Espreafico, P. Forscher, R.E. Larson, and M.S. Mooseker. 1993. Brain myosin-V is a two-headed unconventional myosin with motor activity. *Cell.* 75: 13–23.

Citi, S., and J. Kendrick-Jones. 1987. Regulation of non-muscle myosin structure and function. *Bioessays.* 7:155–159.

Drubin, D.G., and W.J. Nelson. 1996. Origins of cell polarity. *Cell.* 84:335–344.

Dulic, V., M. Egerton, I. Elguindi, S. Raths, B. Singer, and H. Riezman. 1991. Yeast endocytosis assays. *Methods Enzymol.* 194:697–709.

Engebrecht, J., J. Hirsch, and G.S. Roeder. 1990. Meiotic gene conversion and crossing over: their relationship to each other and to chromosome synapsis and segregation. *Cell.* 62:927–937.

Erhart, E., and C.P. Hollenberg. 1983. The presence of a defective *LEU2* gene on 2 μ DNA recombinant plasmids of *Saccharomyces cerevisiae* is responsible for curing and high copy number. *J. Bacteriol.* 156:625–635.

Finger, F.P., T.E. Hughes, and P. Novick. 1998. Sec3p is a spatial landmark for polarized secretion in budding yeast. *Cell.* 92:559–571.

Futcher, A.B., and B.S. Cox. 1984. Copy number and the stability of 2-μm circle-based artificial plasmids of *Saccharomyces cerevisiae*. *J. Bacteriol.* 157: 283–290.

Gary, R., and A. Bretscher. 1995. Ezrin self-association involves binding of an N-terminal domain to a normally masked C-terminal domain that includes the F-actin binding site. *Mol. Biol. Cell.* 6:1061–1075.

Gietz, R.D., and R.H. Schiestl. 1995. Transforming yeast with DNA. *Methods Mol. Cell. Biol.* 5:255–269.

Govindan, B., R. Bowser, and P. Novick. 1995. The role of Myo2, a yeast class V myosin, in vesicular transport. *J. Cell Biol.* 128:1055–1068.

Haarer, B.K., A. Corbett, Y. Kweon, A.S. Petzold, P. Silver, and S.S. Brown. 1996. *SEC3* mutations are synthetically lethal with profilin mutations and cause defects in diploid-specific bud-site selection. *Genetics*. 144:495–510.

Heath, I.B. 1994. The cytoskeleton in hyphal growth, organelle movements and mitosis. *In* The Mycota. Vol. I. J.G.H. Wessels and F. ad Meinhardt, editors. Springer-Verlag, Heidelberg, Germany. 43–65.

Herskowitz, I., and J.E. Jensen. 1991. Putting the *HO* gene to work: practical uses for mating-type switching. *Methods Enzymol.* 194:132–145.

Hill, K.L., N.L. Catlett, and L.S. Weisman. 1996. Actin and myosin function in directed vacuole movement during cell division in *Saccharomyces cerevisiae*. *J. Cell Biol.* 135:1535–1549.

Horn, P., and D. Wilkie. 1966. Use of Magdala red for the detection of auxotrophic mutants of *Saccharomyces cerevisiae*. *J. Bacteriol.* 91:1388.

Huang, J.-D., S.T. Brady, B.W. Richards, D. Stenoien, J.H. Resau, N.G. Copeland, and N.A. Jenkins. 1999. Direct interaction of microtubule- and actin-based transport motors. *Nature.* 397:267–270.

Huffaker, T.C., J.H. Thomas, and D. Botstein. 1988. Diverse effects of beta-tubulin mutations on microtubule formation and function. *J. Cell Biol.* 106: 1997–2010.

Jacobs, C.W., A.E.M. Adams, P.J. Szaniszlo, and J.R. Pringle. 1988. Functions of microtubules in the *Saccharomyces cerevisiae* cell cycle. *J. Cell Biol.* 107: 1409–1426.

Johnston, G.C., J.A. Prendergast, and R.A. Singer. 1991. The *Saccharomyces cerevisiae MYO2* gene encodes an essential myosin for vectorial transport of vesicles. *J. Cell Biol.* 113:539–551.

Keller, P., and K. Simons. 1997. Post-Golgi biosynthetic trafficking. *J. Cell Sci.* 110:3001–3009.

Lillie, S.H., and S.S. Brown. 1992. Suppression of a myosin defect by a kinesin-related gene. *Nature.* 356:358–361.

Lillie, S.H., and S.S. Brown. 1994. Immunofluorescence localization of the unconventional myosin, Myo2p, and the putative kinesin-related protein, Smy1p, to the same regions of polarized growth in *Saccharomyces cerevisiae*. *J. Cell Biol.* 125:825–842.

Lillie, S.H., and S.S. Brown. 1998. Smy1p, a kinesin-related protein that does not require microtubules. *J. Cell Biol.* 140:873–883.

Long, R.M., R.H. Singer, X. Meng, I. Gonzalez, K. Nasmyth, and R.P. Jansen. 1997. Mating type switching in yeast controlled by asymmetric localization of *ASH1* mRNA. *Science.* 277:383–387.

Lupas, A. 1996. Prediction and analysis of coiled-coil structures. *Methods Enzymol.* 266:513–525.

Mermall, V., P.L. Post, and M.S. Mooseker. 1998. Unconventional myosins in cell movement, membrane traffic, and signal transduction. *Science.* 279:527–533.

Mitchell, D.A., T.K. Marshall, and R.J. Deschenes. 1993. Vectors for the inducible overexpression of glutathione S-transferase fusion proteins in yeast. *Yeast.* 9:715–722.

Mooseker, M.S., and R.E. Cheney. 1995. Unconventional myosins. *Annu. Rev. Cell Dev. Biol.* 11:633–675.

Mulholland, J., A. Wesp, H. Riezman, and D. Botstein. 1997. Yeast actin cytoskeleton mutants accumulate a new class of Golgi-derived secretory vesicle. *Mol. Biol. Cell.* 8:1481–1499.

Mulholland, J., J. Konopka, B. Singer-Kruger, M. Zerial, and D. Botstein. 1999. Visualization of receptor-mediated endocytosis in yeast. *Mol. Biol. Cell.* 10: 799–817.

Novick, P., and D. Botstein. 1985. Phenotypic analysis of temperature-sensitive yeast actin mutants. *Cell.* 40:405–416.

Novick, P., C. Field, and R. Schekman. 1980. Identification of 23 complementation groups required for post-translational events in the yeast secretory pathway. *Cell.* 21:205–215.

Parle-McDermott, A.G., N.J. Hand, S.E. Goulding, and K.H. Wolfe. 1996. Sequence of 29 kb around the *PDR10* locus on the right arm of *Saccharomyces cerevisiae* chromosome XV: similarity to part of chromosome I. *Yeast.* 12: 999–1004.

Pearson, B.M., Y. Hernando, J. Payne, S.S. Wolf, A. Kalogeropoulos, and M. Schweizer. 1996. Sequencing of a 35.71 kb DNA segment on the right arm of yeast chromosome XV reveals regions of similarity to chromosomes I and XIII. *Yeast.* 12:1021–1031.

Prekeris, R., and D.M. Terrian. 1997. Brain myosin V is a synaptic vesicle-associated motor protein: evidence for a Ca2+-dependent interaction with the synaptobrevin–synaptophysin complex. *J. Cell Biol.* 137:1589–1601.

Pringle, J.R. 1991. Staining of bud scars and other cell wall chitin with calcofluor. *Methods Enzymol.* 194:732–734.

Pringle, J.R., A.E.M. Adams, D.G. Drubin, and B.K. Haarer. 1991. Immunofluorescence methods for yeast. *Methods Enzymol.* 194:565–601.

Protopopov, V., B. Govindan, P. Novick, and J.E. Gerst. 1993. Homologs of the synaptobrevin/VAMP family of synaptic vesicle proteins function on the late secretory pathway in *S. cerevisiae*. *Cell.* 74:855–861.

Pruyne, D.W., D.H. Schott, and A. Bretscher. 1998. Tropomyosin-containing actin cables direct the Myo2p-dependent polarized delivery of secretory vesicles in budding yeast. *J. Cell Biol.* 143:1931–1945.

Reck-Peterson, S.L., P.J. Novick, and M.S. Mooseker. 1999. The tail of a yeast class V myosin, Myo2p, functions as a localization domain. *Mol. Biol. Cell.* 10:1001–1017.

Santos, B., and M. Snyder. 1997. Targeting of chitin synthase 3 to polarized growth sites in yeast requires Chs5p and Myo2p. *J. Cell Biol.* 136:95–110.

Sassanfar, M., and J.W. Roberts. 1990. Nature of the SOS-inducing signal in *Escherichia coli*. The involvement of DNA replication. *J. Mol. Biol.* 212:79–96.

Schliwa, M. 1999. Molecular motors join forces. *Nature.* 397:204–205.

Schnarr, M., J. Pouyet, M. Granger-Schnarr, and M. Daune. 1985. Large-scale purification, oligomerization equilibria, and specific interaction of the LexA repressor of *Escherichia coli*. *Biochemistry*. 24:2812–2818.

Seiler, S., F.E. Nargang, G. Steinberg, and M. Schliwa. 1997. Kinesin is essential for cell morphogenesis and polarized secretion in *Neurospora crassa*. *EMBO (Eur. Mol. Biol. Organ.) J.* 16:3025–3034.

Sherman, F. 1991. Getting started with yeast. *Methods Enzymol.* 194:3–21.

Sikorski, R.S., and P. Hieter. 1989. A system of shuttle vectors and yeast host strains designed for efficient manipulation of DNA in *Saccharomyces cerevisiae*. *Genetics.* 122:19–27.

Smith, D.B., and K.S. Johnson. 1988. Single-step purification of polypeptides expressed in *Escherichia coli* as fusions with glutathione S-transferase. *Gene.* 67:31–40.

Stoffler, H.E., and M. Bahler. 1998. The ATPase activity of Myr3, a rat myosin I, is allosterically inhibited by its own tail domain and by Ca2+ binding to its light chain calmodulin. *J. Biol. Chem.* 273:14605–14611.

Storms, R.K., Y. Wang, N. Fortin, J. Hall, D.H. Vo, W.W. Zhong, T. Downing, A.B. Barton, D.B. Kaback, Y. Su, and H. Bussey. 1997. Analysis of a 103 kbp cluster homology region from the left end of *Saccharomyces cerevisiae* chromosome I. *Genome.* 40:151–164.

Takizawa, P.A., A. Sil, J.R. Swedlow, I. Herskowitz, and R.D. Vale. 1997. Actin-dependent localization of an RNA encoding a cell-fate determinant in yeast. *Nature.* 389:90–93.

Thompson, J.D., D.G. Higgins, and T.J. Gibson. 1994. CLUSTAL W: improving the sensitivity of progressive multiple sequence alignment through sequence weighting, position-specific gap penalties and weight matrix choice. *Nucleic Acids Res.* 22:4673–4680.

Walch-Solimena, C., R.N. Collins, and P.J. Novick. 1997. Sec2p mediates nucleotide exchange on Sec4p and is involved in polarized delivery of post-Golgi vesicles. *J. Cell Biol.* 137:1495–1509.

Wolfe, K.H., and D.C. Shields. 1997. Molecular evidence for an ancient duplication of the entire yeast genome. *Nature.* 387:708–713.